

Bridging the scales: Short- to long-term
deformation signals from a laboratory subduction
megathrust

Dissertation

zur Erlangung des Grades eines
Doktors der Naturwissenschaften (Dr. rer. nat.)
am Fachbereich Geowissenschaften
der Freien Universität Berlin

vorgelegt von

Ehsan Kosari



Berlin, 2021

Erstgutachter:

Prof. Dr. Onno Oncken

Freie Universität Berlin; GeoForschungsZentrum Potsdam

Zweitgutachter:

Prof. Dr. Francesca Funicello

Roma Tre University, Rome, Italy

Prüfungskommission:

Prof. Dr. Frederik Tilmann, *Freie Universität Berlin; GeoForschungsZentrum Potsdam*

Prof. Dr. Eline Le Breton, *Freie Universität Berlin, Berlin, Germany*

Prof. Dr. Onno Oncken, *Freie Universität Berlin; GeoForschungsZentrum Potsdam*

Prof. Dr. Francesca Funicello, *Roma Tre University, Rome, Italy*

Dr. Jörn Kummerow, *Freie Universität Berlin, Berlin, Germany*

Tag der Disputation: 21.01.2022

Erklärung

nach §7 (4) der Promotionsordnung des Fachbereichs Geowissenschaften and der Freien Universität Berlin:

Hiermit erkläre ich, dass die vorliegende Dissertation ohne unzulässige Hilfe Dritter und ohne Benutzung anderer als der angegebenen Literatur angefertigt wurde. Die Stellen der Arbeit, die anderen Werken wörtlich oder inhaltlich entnommen sind, wurden durch entsprechende Angaben der Quellen kenntlich gemacht. Diese Arbeit hat in gleicher oder ähnlicher Form noch keiner Prüfungsbehörde vorgelegen.

Ehsan Kosari
Berlin, September 2021

And I keep in my mind that
I shall not violate the Law of the Earth.

Sohrab Sepehri, Iranian poet and painter (1928–1980)

Dedication

I would like to dedicate this thesis to all my family members

Acknowledgments

First of all, I would like to thank Prof. Onno Oncken and Dr. Matthias Rosenau for helping me carry out the present thesis, as well as for letting me take the initiative in implementing my own ideas in some parts of this research. Their knowledge, motivation, and patience have been essential throughout this academic journey. I also wish to thank Prof. Niels Hovius and Dr. Michael Dietze for designing and managing the SUBITOP project.

I would like to especially appreciate our laboratory team, Michael Rudolf, Thomas Ziegenhagen, and Frank Neumann, for making a pleasant atmosphere and their great support and discussion during laboratory works. I also would like to thank our student assistants in the HelTec lab, Jan and Andre.

A big “Thank You” goes to Franziska Alberg, Coordinator for Department 4 "Geomaterials" and Lithosphere Dynamics section of the GFZ German Research Centre for Geosciences, who is always an accurate solution for our problems and thinks of our needs before they appear. I also would like to thank our secretaries in the Lithosphere Dynamics section: Antje Schäfer, Regina Prero, and Sandra Paulin. I am also grateful to our colleagues at GFZ welcome center, Frauke Stobbe, Pia Sojka, Lydia Bauer, and from IT section, Heiner Brauer, for always being generously supportive.

I want to thank Dr. Bernd Schurr and Dr. Jonathan Bedford for involving me in the HART (AfterShocks Field Campaign) and the Integrated Plate Boundary Observatory Chile (IPOC) projects during my Ph.D. research; Prof. Tim Wright (from COMET at Leeds), Dr. Richard Jones (GRL Ltd.), Dr. Francesca Funicello and Dr. Fabio Corbi (Roma Tre University) for hosting me during my academic visits. They helped me to grow in additional directions.

Moreover, I want to thank all my friends and colleagues at GFZ: my great office-mate Io Ioannidi and Isabel Urrutia, for the wonderful moments and for making my everyday life happy; Dr. Mehdi Nikkhoo and Dr. Nima Nooshiri for their advice and practical tips during my first year of Ph.D. Dr. Sabrina Metzger for patiently discussing with me some scientific challenges; Armel Menant and Silvia Crosetto for scientific discussions and also random non-scientific chats. I am grateful to Hugo Soto, Begona Parraguez Landaeta, Roman Eugenio Gonzalez, Violeta Veliz-Borel, and all the section members for various interesting conversations.

I acknowledge the Marie Skłodowska-Curie framework. This research has received funding from the European Union's EU Framework Programme for Research and Innovation Horizon 2020 under Grant Agreement No 674899.

Zusammenfassung

In Subduktionszonen, in denen sich eine tektonische Platte unter die andere schiebt, ereignen sich die größten Erdbeben der Erde. Diese Zonen zeichnen sich durch eine starke Erdbeben­­tätigkeit aus und sind für 95 % der Energiefreisetzung durch Erdbeben auf der Erde verantwortlich. Der obere Teil der Subduktionszone (d. h. die *Megathrust*) erzeugte die größten jemals aufgezeichneten Erdbeben wie das Valdivia-Erdbeben von 1960 in Chile, das Sumatra-Erdbeben von 2004 in Indonesien und das Tohoku-Oki-Erdbeben von 2011 in Japan. Die Entschlüsselung des Verhaltens dieses Teils der Subduktionszone, der die bedeutendsten Erdbeben und verheerenden Tsunamis hervorruft, ist ein entscheidender Schritt nach vorn in der Erdbebengeowissenschaft. Die Beobachtung von nur einem Bruchteil eines einzelnen *Megathrust*-Erdbebenzyklus und die Offshore-Lage der Quelle dieser Erdbeben sind die Hauptgründe für das unzureichende Verständnis. Die unzureichende Offshore-Beobachtung und die Unvollständigkeit der interseismischen Daten haben die Erdbebenforscher dazu veranlasst, analoge und numerische Modellierungsansätze anzuwenden, um den Zusammenhang zwischen kurzfristiger elastischer (d. h. koseismischer) und langfristiger permanenter (d. h. mehrere seismische Zyklen umfassender) Verformung der Subduktionszonen aufzudecken. Die Aufdeckung dieser Beziehungen ermöglicht es uns, zu ermitteln, nach welchen lang- und kurzfristigen Signalen Erdbebenforscher suchen sollten, um die seismische Zyklusgeschichte der Subduktionszone zu entschlüsseln.

In dieser Forschungsarbeit untersuche ich ein vereinfachtes analoges Modell einer Subduktionszone vom Tiefsee­­graben bis zum Vulkanbogen und etwa 240 km entlang des Streichens der Subduktionszone unter Verwendung von elastoplastischem granule­­rem Material und analogem Stick-Slip-Material im Labormaßstab. Die Erstellung allgemeiner seismotektonischer Modelle ermöglicht es mir, Hunderte von seismischen *Megathrust*-Erdbebenzyklen zu erzeugen und die erdbebenbedingten Oberflächen- und Querschnittsverformungsmuster mit hoher räumlicher und zeitlicher Auflösung zu überwachen. Ich versuche zu demonstrieren, welche Oberflächendeformationssignale die Reibung und die mechanischen Veränderungen an der Grenzfläche über koseismische und frühe postseismische Phasen und interseismische Intervalle hinweg erzeugen. Darüber hinaus untersuche ich auf einer längeren Zeitskala (Dutzende bis Hunderte von Erdbebenzyklen), welche Oberflächendeformationsmuster im *Forearc*, vom Graben bis zur Küstenregion, dauerhaft erhalten werden können. Dies liefert den Erdbebengeowissenschaftlern wichtige Beobachtungen, um die Oberflächendeformation des Plattenrandes mit den elastoplastischen Prozessen unter der Oberfläche im flachen Teil der Subduktionsgrenze zu verbinden.

Ich wende eine geodätische Inversionstechnik zur Ableitung des koseismischen Versatzes entlang der *Megathrust* auf analoge grabenbrechende und nicht grabenbrechende *Megathrust* Erdbeben an, um zu demonstrieren, wie eine begrenzte geodätische *Offshore*-Abdeckung

koseismische Versatzmodelle beeinflusst. Die aus analogen Erdbeben abgeleiteten Versatzmodelle zeigen quantitative und qualitative Veränderungen in Abhängigkeit von der *Offshore*-Abdeckung: 1) Flacher Versatz kann nicht aufgelöst werden, wenn die Beobachtungsabdeckung des *Offshore*-Segments $<50\%$ ist. 2) Das Versatzmuster eines flachen Ereignisses kippt von landwärts zu grabenwärts vergent, wenn die *Offshore*-Abdeckung auf $<40\%$ sinkt. 3) Im Falle keiner küstennahen Abdeckung konvergiert das Versatzmuster für beide Ereignistypen zu einem ähnlichen unimodalen Muster. Darüber hinaus schließe ich auf eine 5-20%ige Überschätzung des Versatzes, wenn die Beobachtungen oberhalb der flachen Versatzzone während grabenbrechenden Ereignissen liegen, gegenüber einer 5-10%igen Unterschätzung während nicht grabenbrechenden Ereignissen, wenn die Beobachtungen landgebunden sind. Außerdem kann die für grabenbrechende Brüche abgeleitete Momentgröße beeinflusst werden.

Darüber hinaus ahme ich homogene und heterogene *Megathrust*-Grenzflächen im Labormaßstab nach, um die Dehnungsrelaxation an den beiden elastisch nicht identischen Platten zu überwachen, indem ich analoge Materialien einsetze, die ratenabhängige Festigkeiten zeigen. Ich schlage einen sequentiellen elastischen *Rebound* vor, der dem koseismischen Scherspannungsabfall in den elastischen Reibungsmodellen folgt: einen schnellen *Rebound* der oberen Platte und den verzögerten und kleineren *Rebound* an der abtauchenden Platte. Der verzögerte *Rebound* der abtauchenden Platte, zusammen mit der schnellen Entspannung der oberen Platte nach einem elastischen Überschießen, beschleunigt die Wiederkopplung der *Megathrust*. Diese Beschleunigung löst/begünstigt das Versagen einer nahe gelegenen *Asperity* und verstärkt das frühe Rückgleiten im Bruchbereich.

Die langfristige reibungs-elastoplastische Wechselwirkung zwischen der Grenzfläche und dem darüber liegenden Keil verursacht variable Oberflächendehnungssignale. Ich habe zwei Keilkonfigurationen mit koseismischer Kompression und Dehnung erstellt, um die mechanische und kinematische Wechselwirkung zwischen dem flachen Keil und der Grenzfläche zu untersuchen. Die Ergebnisse zeigen, dass diese Wechselwirkung den Keil in verschiedene Segmente aufteilen kann. Ich hebe hervor, dass eine stärker segmentierte obere Platte eine Subduktions-*Megathrust* darstellt, die mehr charakteristische und periodische Ereignisse erzeugt. Darüber hinaus veranschaulichen die Ergebnisse, dass verschiedene Keilsegmente ihren Zustand von Kompressions-/Dehnungs- zu Extensions-/Kompressionsbereichen wechseln können. Darüber hinaus zeigt die Zeitreihe der Dehnungen in der Küstenzone, dass der Dehnungszustand über einige seismische Zyklen quasistabil bleiben kann, bevor er in einen entgegengesetzten Verkürzungs-Modus übergeht. Diese Beobachtungen sind von entscheidender Bedeutung für die Bewertung erdbebenbedingter morphotektonischer Marker (z. B. Meeresterrassen) und kurzfristiger interseismischer GPS-Zeitserien an Land (Küstenregion).

Summary

Subduction zones, where one tectonic plate slides underneath the other, host the largest earthquakes on Earth. These zones are characterized by intense earthquake activity and are responsible for 95 % of all moment releases on Earth. The shallow portion of the subduction zone interface (i.e., megathrust) generated the largest ever recorded earthquakes, such as the 1960 Valdivia earthquake in Chile, the 2004 Sumatra earthquake in Indonesia, and the 2011 Tohoku-Oki earthquake in Japan on the Earth. Unwrapping the behavior of this portion of the subduction zone, which generates the most significant earthquakes and devastating tsunamis, is a vital step forward in earthquake geoscience. Monitoring only a fraction of a single megathrust earthquake cycle and the offshore location of the source of these earthquakes are the foremost reasons for the insufficient understanding. The insufficient offshore observation and the interseismic data incompleteness led earthquake scientists to employ analog and numerical modeling approaches to unfold the linkage between short-term elastic (i.e., coseismic) and long-term permanent (i.e., several seismic cycles) deformation of the subduction zones. Revealing these relationships allows us to identify which long and short-term signals earthquake scientists should look for remotely or in the field to unwrap the subduction zone's seismic cycle history.

In this research, I investigate a simplified analog model of a subduction zone from trench to the location of volcanic arc and 240 km along strike using elastoplastic granular material and stick-slip analog material at a laboratory scale. Establishing generic seismotectonic scale models enables me to generate hundreds of megathrust seismic cycles and monitor the earthquake-related surface and cross-sectional deformation pattern at high resolution in both space and time. I attempt to demonstrate what surface deformation signals the frictional and mechanical changes on the interface generates over coseismic and early postseismic stages and interseismic intervals. Additionally, at a more extended time scale (tens to hundreds of earthquake cycles), I study what surface strain pattern in the forearc from trench to the coastal region can be permanently preserved. This provides critical observations for earthquake geoscientists to tie

forearc surface deformation to subsurface elastoplastic processes at the shallow portion of the subduction interface.

I apply a geodetic slip inversion technique to analog trench-breaking and non-trench-breaking megathrust earthquakes to demonstrate how limited offshore geodetic coverage affects coseismic slip models. The slip models derived from analog earthquakes show quantitative and qualitative changes as a function of offshore coverage: 1) Shallow slip cannot be resolved if the observation coverage of the offshore segment is <50%. 2) the slip pattern of shallow event flips from landward to trenchward skewed as offshore coverage reduces to <40%. 3) In the case of no offshore coverage, the slip pattern for both event types converges to a similar unimodal pattern. Additionally, I infer 5-20% slip overestimation when the observations are above the high slipping zone during trench-breaking events versus 5-10% underestimation during non-trench-breaking events if observations are land-limited. Moreover, the moment magnitude derived for trench-breaking ruptures might be affected.

Furthermore, I mimic homogenous and heterogeneous megathrust interfaces at the laboratory scale to monitor the strain relaxation on the two elastically non-identical plates by establishing analog velocity weakening and strengthening materials. I propose a sequential elastic rebound that follows the coseismic shear-stress drop in the elastic-frictional models: a fast rebound of the upper plate and the delayed and smaller rebound on the slab. The delayed rebound of the slab, along with the rapid relaxation of the upper plate after an elastic overshooting, accelerates the relocking of the megathrust. This acceleration triggers/antedates the failure of a nearby asperity and enhances the early backslip in the rupture area.

The long-term frictional-elastoplastic interaction between the interface and its overlying wedge causes variable surface strain signals. I establish two coseismically compressional and extensional wedge configurations to explore the mechanical and kinematic interaction between the shallow wedge and the interface. The results demonstrate that this interaction can partition the wedge into different segments. I highlight that a more segmented upper plate represents a subduction megathrust that generates more characteristic and periodic events. Moreover, the results illustrate that different wedge segments may switch their state from compression/extension to extension/compression domains. Additionally, the strain time series of the coastal zone reveals that the strain state may remain quasi-stable over a few seismic cycles before switching to the opposite mode. These observations are key for evaluating earthquake-related morphotectonic markers (i.e., marine terraces) and short-term interseismic GPS time-series onshore (coastal region).

Contents

1	Chapter 1: Introduction	1
1.1	Thesis objectives and outline.....	2
1.2	Plate tectonic concept	5
1.3	Earthquakes in subduction zones.....	6
1.4	Megathrust seismic cycle.....	8
1.5	Experimental approaches overview	11
1.6	Model Scaling and similarity.....	12
1.6.1	Interseismic phase scaling	13
1.6.2	Coseismic phase scaling	14
1.7	The Rate-and-State Framework.....	15
1.8	Analog materials and experimental setup.....	17
1.8.1	Laboratory geodesy	18
1.8.2	Inversion Procedure.....	18
1.9	References:	20
2	Chapter 2: On the relationship between offshore geodetic coverage and slip model uncertainty: Analog megathrust earthquake case studies.....	26
2.1	Abstract.....	27
2.2	Introduction	27
2.3	Methodology.....	27
2.3.1	Seismotectonic scale modeling	27
2.3.2	Surface deformation monitoring	27
2.3.3	Inversion procedure.....	27
2.4	Results of the inversions with limited offshore geodetic coverage	27
2.4.1	Effect on fault recoverability.....	27
2.4.2	Effects on slip pattern and peak slip.....	27
2.4.3	Effects on rupture limits and centroid location	27
2.4.4	Effects on seismic moment and magnitude.....	27
2.5	Discussion.....	27
2.6	Conclusions	27

2.7	References	27
2.8	Supporting Information for chapter 2	27
3	Chapter 3: Postseismic backslip as a response to a sequential elastic rebound of upper plate and slab in subduction zones	64
3.1	Abstract.....	65
3.2	Introduction	65
3.3	Methodology.....	65
3.3.1	Seismotectonic scale modeling	65
3.3.2	Laboratory geodesy	65
3.4	Results: Observations and interpretations	65
3.4.1	Time-variable surface displacements and slip over an analog earthquake and the early postseismic	65
3.4.2	Coulomb failure stress changes.....	65
3.4.3	Elastic rebound of upper plate and slab	65
3.4.4	Upper plate displacement accumulation	65
3.5	Discussion and conclusion.....	65
3.5.1	Effect of the slab acceleration on the rapid relocking	65
3.5.2	Effects of the acceleration on event triggering.....	65
3.6	References	65
3.7	Supporting Information for Chapter 3	65
4	Chapter 4: Strain signals governed by frictional-elastoplastic interaction of the upper plate and shallow subduction megathrust interface over seismic cycles	92
4.1	Abstract.....	93
4.2	Introduction	93
4.3	Seismotectonic Scale Modeling and Monitoring Techniques	93
4.4	Results and Interpretations	93
4.4.1	Model Evolution from long to short timescales	93
4.4.2	Frequency and size distributions of analogue megathrust events	93
4.5	Discussion.....	93
4.5.1	Mechanical state of the shallow forearc over the seismic cycle.....	93
4.5.2	Seismotectonic forearc segmentation: Comparison with natural examples.....	93
4.5.3	Forearc segmentation and temporal pattern of events.....	93
4.5.4	Coastal strain cycle in response to earthquake cycle	93
4.6	Conclusion	93
4.7	References	93
4.8	Supporting Information for Chapter 4	93

5	Chapter 5: Conclusions and outlook	129
5.1	Conclusions and outlook	130
5.1.1	Conclusions	130
5.1.2	Outlook.....	131
6	Curriculum Vitae	133

LIST OF MAIN FIGURES

FIGURE 1- 1:	COSIESMIC AND EARLY-POSTSEISMIC SURFACE DEFORMATION PATTERN IN THE DIRECTION OF THE LINE OF SIGHT DERIVED FROM DIFFERENT LARGE EARTHQUAKES IN THE CHILEAN SUBDUCTION ZONE: A) SENTINEL-1 UNWRAPPED INTERFEROGRAM OF THE 2015 ILLAPEL EARTHQUAKE (Mw 8.3). B) RADARSAT2 UNWRAPPED INTERFEROGRAM OF THE IQUIQUE 2014 EARTHQUAKE (Mw 8.2 (HOFFMANN ET AL. 2018)). C) ENVISAT UNWRAPPED INTERFEROGRAM OF THE 2007 TOCOPILLA EARTHQUAKE (Mw 7.8) (MOTAGH ET AL. 2010).....	3
FIGURE 1- 2:	LOCATION OF THE SUBDUCTION ZONES AND THEIR GEOMETRY (HAYES ET AL. 2018) AND THE DISTANCE FROM TRENCH TO THE COASTLINE (BLUE BAR CHARTS) IN DIFFERENT SUBDUCTION ZONES (MALATESTA ET AL. 2021).....	4
FIGURE 1- 3:	EARTH SEISMICITY MAP. THE EPICENTER OF THE EARTHQUAKES WITH MAGNITUDES EQUAL AND LARGER THAN 6 IN THE PERIOD FROM 1900 TO 2021 IS OVERLAYED ON THE WORLD SRTM30 DIGITAL ELEVATION MODEL. NOTE THAT MAJORITY OF THE LARGE EARTHQUAKES ARE CONCENTRATED IN THE SUBDUCTION ZONES.	6
FIGURE 1- 4:	CROSS-SECTION OF A SUBDUCTION ZONE SHOWING THE DIFFERENT TYPES OF EARTHQUAKE MECHANISMS. THE SHALLOW EXTENSIONAL EARTHQUAKES OCCUR IN THE OUTER-RISE IN THE SUBDUCTING PLATE. THE UPPERMOST AREA OF THE INTERFACE IS DOMINATED BY SHALLOW MEGATHRUST EARTHQUAKES CAUSED BY HORIZONTAL COMPRESSION. DEWATERING CAUSES INTERMEDIATE EARTHQUAKES TO DEPTHS OF 400 KM. DEEP EARTHQUAKES ARE PROBABLY CREATED BY THE MINERAL PHASE TRANSITION IN DEPTHS BETWEEN 350 AND 700 KM (FRISCH ET AL. 2010; GREEN 1994).	7
FIGURE 1- 5:	SIMPLIFIED OVERVIEW OF DIFFERENT PHASES OF AN EARTHQUAKE CYCLE (HICKS 2015).....	8
FIGURE 1- 6:	A: NEAR-TRENCH DOMAIN WHERE TSUNAMI EARTHQUAKES OR ANELASTIC DEFORMATION AND STABLE SLIDING OCCUR; B: CENTRAL MEGATHRUST DOMAIN WHERE LARGE SLIP OCCURS WITH MINOR SHORT-PERIOD SEISMIC RADIATION; C: DOWNDIP DOMAIN WHERE MODERATE SLIP OCCURS WITH SIGNIFICANT COHERENT SHORT-PERIOD SEISMIC RADIATION; D: TRANSITIONAL DOMAIN WHERE SLOW SLIP EVENTS, LOW-FREQUENCY EARTHQUAKES (LFES), AND SEISMIC TREMOR CAN OCCUR (LAY ET AL. 2012)....	9
FIGURE 1- 7:	SIMPLIFIED SEISMIC CYCLE ON A SUBDUCTION ZONE. DISPLACEMENTS AT DEPTH, INDICATED BY RED ARROWS (COSEISMIC) AND BLUE ARROWS (CUMULATED OVER THE INTERSEISMIC PERIOD). THE SHALLOWER PORTION OF THE MEGATHRUST, HIGHLIGHTED IN RED, SLIPS ONLY DURING TRANSIENT SLIP EVENTS (INTERPLATE EARTHQUAKES, AFTERSLIP, OR SLOW SLIP EVENTS) AND IS FULLY LOCKED DURING THE INTERSEISMIC PERIOD. B: DISPLACEMENTS AT THE SURFACE: THE RED LINE REPRESENTS THE SURFACE DISPLACEMENT RATE RELATIVE TO THE STABLE OVERRIDING PLATE. THE BLUE LINE REPRESENTS THE LONG-TERM SURFACE DISPLACEMENT RATE. THE DIFFERENCE BETWEEN THE TWO CURVES, DEPICTED BY THE LIGHT GREEN LINE, REPRESENTS THE CONTRIBUTION OF TRANSIENT SLIP EVENTS (AVOUAC 2015).	10
FIGURE 1- 8:	PRIMARY PROCESSES AFTER A SUBDUCTION EARTHQUAKE. 1) ASEISMIC AFTERSLIP AROUND THE RUPTURE ZONE, (2) VISCOELASTIC RELAXATION, AND (3) RELOCKING (WANG, HU, AND HE 2012B).....	11
FIGURE 1- 9:	DIFFERENT TYPES OF EXPERIMENTAL ANALOG MODELS: A) SPRING-SLIDER MODEL (v IS VELOCITY, ΣN IS NORMAL LOAD, AND μ IS FRICTION COEFFICIENT); B) FAULT BLOCK MODEL; (C) SEISMOTECTONIC SCALE MODEL (A–B IS RATE–STATE PARAMETER, H IS VISCOSITY, G IS GRAVITATIONAL ACCELERATION, AND V IS FORCE (ROSENAU ET AL. 2017B).	12
FIGURE 1- 10:	SCHEMATIC DIAGRAM DEFINING THE TERMS IN THE RATE–STATE FRICTION LAW (C. H. SCHOLZ 1998).....	16
FIGURE 1- 11:	EXPERIMENTAL RESULTS FROM SLIDE-HOLD-SLIDE TESTS (MARONE 1998). (A): THE STRENGTH OF THE FAULT ZONE INCREASES WITH INCREASING HOLD TIME. (B): TYPICAL CURVE OF A SLIDE-HOLD-SLIDE	

TEST SHOWING RELOADING PEAKS AFTER 100 s AND 10 s. (C): THE VELOCITY WEAKENING BEHAVIOR OF FAULT GOUGES AND ROCK SURFACES. (D): EVOLUTION OF FRICTION DURING A VELOCITY STEPPING TEST (RUDOLF 2019). 17

FIGURE 2- 1: CHECKERBOARD TEST FOR TRENCH-BREAKING A-B (A-C) AND NON-TRENCH-BREAKING B-C (D-F) TYPE EVENTS. THE MAGENTA AND YELLOW MARKERS INDICATE THE OFFSHORE AND ONSHORE vGNSSs STATIONS, RESPECTIVELY. THE RESULTS ARE VISUALIZED AS THE DIFFERENCE BETWEEN THE TARGET (SYNTHETIC) SLIP AND THE INVERTED SLIP. NOTE THAT THE NUMBER OF MARKERS IS SMALLER THAN THE NUMBER OF DIGITAL IMAGE CORRELATION DERIVED MEASUREMENTS REALIZED IN THE EXPERIMENTS FOR REASONS OF VISUALIZATION. THE TARGET SLIP CAN BE FOUND IN FIGURE S4..... 27

FIGURE 2- 2: EXAMPLES OF SLIP PATTERNS AND THEIR SENSITIVITY TO OFFSHORE GEODETIC COVERAGE: TRENCH-BREAKING A-B (A-C) VERSUS NON-TRENCH-BREAKING B-C TYPE EVENTS (D-F). THE GRAY AND MAGENTA MARKERS REPRESENT THE vGNSSs COVERAGE OF ONSHORE AND OFFSHORE, SEPARATELY..... 27

FIGURE 2- 3: EXAMPLES OF SLIP DISTRIBUTIONS ACROSS AND ALONG STRIKE OF THE SUBDUCTION ZONE AND THEIR SENSITIVITY TO OFFSHORE GEODETIC COVERAGE: TRENCH-NORMAL TRANSECT (A-B) AND TRENCH-PARALLEL TRANSECTS (C-D); TRENCH-BREAKING (A-B) TYPE EVENT VERSUS NON-TRENCH-BREAKING (B-C) TYPE EVENT..... 27

FIGURE 2- 4: SENSITIVITY TO OFFSHORE GEODETIC COVERAGE OF THE LOCATIONS OF THE ANALOG EARTHQUAKE CENTROID (CD, 50TH PERCENTILE OF THE CUMULATIVE SLIP DISTRIBUTION; SEE FIGURES S8, S9, AND S13), ITS DOWN-DIP (DD, ~10TH PERCENTILE), AND UP-DIP (UD, ~90TH PERCENTILE) RUPTURE LIMITS FOR A-B (A) AND B-C (B) TYPE EVENTS, AND OF THE ESTIMATED SEISMIC MOMENTS OF BOTH TYPES OF EVENTS (C). SHOWN ARE MEAN VALUES (SOLID LINE) AND 1 SIGMA STANDARD-DEVIATIONS (SHADED AREA) FOR ALL EVENTS ANALYZED IN THIS STUDY. 27

FIGURE 3-1: MODEL SETUP AND EXEMPLARY EVOLUTION OF COSEISMIC AND EARLY-POSTSEISMIC SURFACE DEFORMATION IN TWO SCENARIOS. A AND B: PLAN VIEW OF THE SEISMOTECTONIC SCALE MODELS' CONFIGURATIONS (FIGURE S1); LIGHT, MEDIUM, AND DARK GRAY COLORS REPRESENT THE VELOCITY STRENGTHENING ("ASEISMICALLY" CREEPING) INTERFACE, A VELOCITY WEAKENING MATRIX CHARACTERIZED BY MICROSLEIPS ("MICROSEISMICITY"), AND THE MAIN SLIP PATCH(ES) (MSP) WHERE LARGE ANALOG MEGATHRUST EARTHQUAKE SLIP OCCURS ("SEISMOGENIC ZONE" OR "ASPERITY"), RESPECTIVELY. THE RED DASHED LINES SHOW THE PROFILES ALONG WHICH THE CUMULATIVE SURFACE DISPLACEMENT IS SHOWN IN C AND D. THE DOWNWARD VECTORS INDICATE SURFACE DISPLACEMENT REVERSAL DURING THE EARLY-POSTSEISMIC STAGE INTERPRETED AS BACKSLIP. THE STARS ON THE DASHED LINES SHOW THE SELECTED SNAPSHOTS FOR SLIP MODELING IN FIGURE 2..... 65

FIGURE 3-2: UPPER PANEL: SLIP MODELS OF THE SELECTED INCREMENTS (MARKED IN FIGURE 1D) IN THE HETEROGENEOUS SYSTEM FOR DEMONSTRATING SLIP/BACKSLIP DISTRIBUTION IN THE MSPS AND THE ANTITHETIC UPPER PLATE FAULT. THE VECTORS INDICATE THE RELATIVE SENSE OF SLIP BUT ARE NOT TO SCALE. THE LOWER PANEL REPRESENTS THREE TRENCH-NORMAL PROFILES OF COULOMB FAILURE STRESS CHANGES (ΔCFS) FROM THE SLIP MODEL SNAPSHOT #12 IN THE HETEROGENEOUS CONFIGURATION. INSET SHOWS THE LOCATION OF PROFILES ON THE MODEL SURFACE. 65

FIGURE 3-3: UPPER PLATE TIME-SERIES OVERLAYED ON THE SLAB TIME-SERIES (BACKGROUND COLORMAP) FROM THE HETEROGENEOUS CONFIGURATION (SEE FIGURE S5 FOR THE HOMOGENOUS CONFIGURATION). NOTE THE LOCATION OF THE PROFILES RELATIVE TO THE UPPER PLATE AND SLAB. THE VERTICAL LINES (E1-E22) INDICATE ABRUPT SURFACE DISPLACEMENT CHANGES ABOVE THE MATRIX. THE WARM COLOR SHOWS LANDWARD DISPLACEMENT OF THE SLAB. LARGER EVENTS INSTIGATE GREATER SLAB RESPONSES (FIGURE S6). 65

FIGURE 3- 4: TIMING OF COSEISMIC AND POSTSEISMIC ELASTIC RESPONSES OF THE UPPER PLATE AND SLAB FOR A REPRESENTATIVE EVENT. A: RELATIVE LOCATION OF THE TIME-SERIES ON BOTH PLATES SHOWN AS ZONE INDEX; B: THE ELASTIC RESPONSE OF THE UPPER-PLATE. T1 TO T3 INDICATES THE RELATIVE TIMING OF THE EVENTS; C: THE ELASTIC RESPONSE OF THE SLAB. 65

FIGURE 4- 1: A: GENERALIZED SHALLOW PORTION OF THE SUBDUCTION ZONE. THE STRUCTURES IN THE UPPER PLATE AND SUBDUCTING PLATE ARE SIMPLIFIED. THIS SCHEMATIC HAS BEEN CONSIDERED AS A BASE FOR OUR ANALOG SEISMOTECTONIC MODEL. B: LABORATORY VIEW OF OUR EXPERIMENT. THE MAIN PART OF THE ANALOG MODEL IS LABELED IN THE IMAGE. C: 2D VIEW OF THE TWO EVALUATED CONFIGURATIONS IN THIS STUDY. THE PROJECTION OF THE DOWN-DIP LIMIT OF THE STICK-SLIP MATERIALS IS DEFINED AS THE

COASTAL AREA. ALPHA (α) AND BETA (β) REPRESENT THE SURFACE AND BASAL DECOLLEMENT, RESPECTIVELY.....	93
FIGURE 4- 2: MECHANICAL STATES OF A WEDGE INTRODUCED BY THE CRITICAL TAPER THEORY FOR COSEISMICALLY COMPRESSIONAL AND EXTENSIONAL EXPERIMENTS. THE AREAS WITHIN THE ENVELOPES CHARACTERIZE STABLE REGIMES. THE AREAS ABOVE AND BELOW THE ENVELOPES INDICATE UNSTABLE EXTENSIONAL AND COMPRESSIONAL REGIMES, RESPECTIVELY. THE POSITIONS ON THE ENVELOPES REPRESENT CRITICALLY STABLE DOMAINS.	93
FIGURE 4- 3: EARTHQUAKE CATALOG DERIVED FROM SURFACE DISPLACEMENT ABOVE THE STICK-SLIP ZONE ON THE MODEL SURFACE. THE DISPLACEMENTS LARGER THAN APPROXIMATELY 0.05 MILLIMETERS REPRESENT AN ANALOG MEGATHRUST EVENT ($M_w \geq 8$ AT NATURE SCALE). DISTANCE BETWEEN TWO ANALOG EVENTS REPRESENTS THE INTERSEISMIC PERIOD IN OUR EXPERIMENTS. A AND B: ALL THE EVENTS THAT OCCURRED OVER MODEL EVOLUTION FROM COMPRESSIONAL AND EXTENSIONAL EXPERIMENTS, RESPECTIVELY. TEMPORAL PROCESSING WINDOWS FOR THREE DIFFERENT RESOLUTIONS ARE DIFFERENTIATED BY SCALE BARS (SEE FIGURES 7 AND 8 FOR MORE DETAILS).C AND D: A SELECTED SET OF 30-32 ANALOG MEGATHRUST EVENTS FOR EVALUATING SURFACE DISPLACEMENT OVER THE SEISMIC CYCLES FROM BOTH CONFIGURATIONS, RESPECTIVELY.	93
FIGURE 4- 4: SURFACE HORIZONTAL DISPLACEMENT (A AND C) AND STRAIN (B AND D) MAPS DERIVED FROM THE EXTENSIONAL CONFIGURATION. THE UPPER PANEL REPRESENTS THE CASE OF A MEGATHRUST EVENT IN WHICH SLIP PROPAGATES ON THE SPLAY FAULTS (NON-TRENCH-REACHING). THE LOWER PANEL REPRESENTS A MEGATHRUST EVENT IN WHICH THE SLIP REACHES THE TRENCH (TRENCH-REACHING SLIP). THE COMPRESSIONAL (OUTER-WEDGE) AND EXTENSIONAL (INNER-WEDGE) SEGMENTS.....	93
FIGURE 4- 5:FINAL SURFACE TOPOGRAPHY OF COMPRESSIONAL (A) AND EXTENSIONAL (B) CONFIGURATIONS. BACKTHRUST AND THE SPLAY FAULTS ARE ROOTED IN THE DOWN-DIP AND UP-DIP LIMIT OF THE STICK-SLIP ZONE. THE SPLAY FAULTS SEPARATE THE OUTER-WEDGE FROM THE INNER-WEDGE. THE STRAIN FIELD GENERATED BY THE ACTIVITY OF THE SPLAY FAULTS IS VISUALIZED IN C. THE RIDGE-SHAPE STRUCTURE REPRESENTS EXTENSIONAL STRAIN. EXAMPLES OF THE SURFACE COSEISMIC EXTENSIONAL FRACTURE ARE SHOWN IN D AND E.....	93
FIGURE 4- 6: FINAL SURFACE DEFORMATION MAPS FROM COMPRESSIONAL (A AND C) AND EXTENSIONAL (B AND D) CONFIGURATIONS. THE APPROXIMATE LOCATION OF THE STICK-SLIP ZONE AT DEPTH IS PROJECTED ON THE MODEL SURFACE AS A DASHED RECTANGLE. A AND B: SURFACE STRAIN MAPS FROM BOTH CONFIGURATIONS. GREEN AND BLUE REPRESENT COMPRESSION AND EXTENSIONAL DOMAINS, RESPECTIVELY. THE OUTER-WEDGE IS EXPERIENCED (SPLAY FAULT AND TRENCH DOMAINS) COMPRESSION. INNER-WEDGE IS RECORDED PERMANENT EXTENSION. THE ACTIVITY OF THE BACKTHRUST IS EVIDENT IN THE COMPRESSIONAL CONFIGURATIONS. C AND D: PERMANENT VERTICAL DEFORMATION IN THE ABSENCE OF EROSION IN THE SYSTEM. THE OUTER- AND INNER-WEDGE REPRESENT PERMANENT SUBSIDENCE AND UPLIFT, RESPECTIVELY. THE SLIGHT SUBSIDENCE ZONE ONSHORE MAY REPRESENT A FOREARC BASIN AT THE NATURAL SCALE.	93
FIGURE 4- 7: INCREMENTAL SURFACE VERTICAL DISPLACEMENT AND STRAIN OVER TIME FROM THE COMPRESSIONAL CONFIGURATION WITH DIFFERENT TEMPORAL RESOLUTIONS (3, 9, AND 18 ANALOG EARTHQUAKE CYCLES). UP-DIP (U.D.) AND DOWN-DIP (D.D.) OF THE STICK-SLIP ZONE AT DEPTH HAVE BEEN PROJECTED ON THE SURFACE. A-C REPRESENTS VERTICAL UPLIFT (WARM COLOR) AND SUBSIDENCE (COLD COLOR). THE ACTIVITY OF THE SPLAY FAULT (S.F.) IS EVIDENT WHILE IT IS GRADUALLY DEACTIVATED AND THE WHOLE SLIP IS TRANSFERRED ON THE MEGATHRUST. D-F REPRESENTS SURFACE STRAIN MAPS WITH DIFFERENT TEMPORAL RESOLUTIONS.	93
FIGURE 4- 8: INCREMENTAL SURFACE VERTICAL DISPLACEMENT AND STRAIN OVER TIME FROM AN EXTENSIONAL CONFIGURATION WITH DIFFERENT TEMPORAL RESOLUTIONS (3, 9, AND 18 ANALOG EARTHQUAKE CYCLES). UP-DIP (U.D.) AND DOWN-DIP (D.D.) OF THE STICK-SLIP ZONE AT DEPTH HAVE BEEN PROJECTED ON THE SURFACE. A-C REPRESENTS VERTICAL UPLIFT (WARM COLOR) AND SUBSIDENCE (COLD COLOR). THE ACTIVITY OF THE SPLAY FAULT (S.F.) IS EVIDENT WHILE IT IS GRADUALLY DEACTIVATED AND THE WHOLE SLIP IS TRANSFERRED ON THE MEGATHRUST. D-F REPRESENTS SURFACE STRAIN MAPS WITH DIFFERENT TEMPORAL RESOLUTIONS.	93
FIGURE 4- 9: COMPRESSIONAL CONFIGURATION; TRENCH-NORMAL DISPLACEMENT TIME-SERIES (RED PLOT) IS OVERLAYED ON THE STRAIN TIME-SERIES (BACKGROUND COLOR MAP) OVER TENS OF ANALOG EARTHQUAKE CYCLES IN DIFFERENT SEGMENTS OF THE UPPER PLATE. THE MAGNITUDE OF THE STRAIN IN THE OUTER-WEDGE IS ONE ORDER LARGER THAN THE INNER-WEDGE AND COAST. NOTE THAT THE OUTER- AND INNER-WEDGE SHOW OPPOSITE STRAIN STATE OVER THE EARTHQUAKE CYCLE (COMPRESSIONAL VERSUS	

EXTENSIONAL). THE COMPRESSION AND EXTENSIONAL SUPERCYCLES IN THE COASTAL REGION ARE SHOWN IN THE LOWER PANEL. PLEASE SEE THE TEXT FOR THE DISCUSSION. 93

FIGURE 4- 10: EXTENSIONAL CONFIGURATION; TRENCH-NORMAL DISPLACEMENT TIME-SERIES (RED PLOT) IS OVERLAYED ON THE STRAIN TIME-SERIES (BACKGROUND COLOR MAP) OVER TENS OF ANALOG EARTHQUAKE CYCLES IN DIFFERENT SEGMENTS OF THE UPPER PLATE. THE MAGNITUDE OF THE STRAIN IN THE OUTER-WEDGE IS ONE ORDER LARGER THAN THE INNER-WEDGE AND COAST. NOTE THAT THE OUTER- AND INNER-WEDGE SHOW OPPOSITE STRAIN STATE OVER THE EARTHQUAKE CYCLE (COMPRESSIONAL VERSUS EXTENSIONAL). THE COMPRESSION AND EXTENSIONAL SUPERCYCLES IN THE COASTAL REGION ARE SHOWN IN THE LOWER PANEL. PLEASE SEE THE TEXT FOR THE DISCUSSION. 93

FIGURE 4- 11: COMPARISON BETWEEN SURFACE DISPLACEMENTS (HORIZONTAL AND VERTICAL) IN THE INNER-WEDGE AND COAST SEGMENTS. THE SEGMENTS DEMONSTRATE OPPOSITE TRENDS: THE COAST MOVES TRENCHWARD WHILE SUBSIDING (AND VICE VERSA), BUT THE INNER-WEDGE MOVES TRENCHWARD WHILE MOVING UPWARD. 93

FIGURE 4- 12: SIZE AND FREQUENCY DISTRIBUTIONS (A AND B) AND COEFFICIENTS OF VARIATION (CV) OF RECURRENCE INTERVALS AND SIZE (C AND D) OF ANALOG MEGATHRUST EVENTS FOR COMPRESSIONAL AND EXTENSIONAL CONFIGURATIONS. 93

FIGURE 4- 13: SUGGESTED SCENARIO FOR THE COASTAL SEGMENT OF THE UPPER PLATE BEHAVIOR OVER TENS OF SEISMIC CYCLES. AFTER EXCEEDING THE ELASTIC DOMAIN, THE UPPER PLATE AT THE LOCATION OF THE COAST GOES TO THE STRAIN-HARDENING DOMAIN OVER A FEW SEISMIC CYCLES AND THEN MOVES TOWARDS THE STRAIN-SOFTENING DOMAIN. THE PULSES OF MEGATHRUST EVENTS (LOADING AND UNLOADING) ACCELERATE THIS SWITCH FROM STRAIN-HARDENING TO STRAIN-SOFTENING. 93

FIGURE 4- 14: SCHEMATIC OF VERTICAL DISPLACEMENT AND STRAIN STATE DURING COSEISMIC PERIOD AND INTERSEISMIC INTERVAL IN DIFFERENT SEGMENTS OF UPPER PLATES FOR DIFFERENT SCENARIOS. NOTE THAT WE ASSUME THE COAST REFLECTS THE DOWN-DIP LIMIT OF THE SEISMOGENIC ZONE AT DEPTH; MODIFIED AFTER (CLARK ET AL., 2019; FARIÁS ET AL., 2011; HERMAN & GOVERS, 2020; MADELLA & EHLERS, 2021; MELNICK ET AL., 2018; MENANT ET AL., 2020; M. S. MORENO, BOLTE, KLOTZ, & MELNICK, 2009; MOUSLOPOULOU ET AL., 2016; OZAWA ET AL., 2011; ROSENAU & ONCKEN, 2009B; SIMONS ET AL., 2011B; SUN, WANG, FUJIWARA, KODAIRA, & HE, 2017B; WANG ET AL., 2019; WANG & TRÉHU, 2016) AND MANY OTHERS..... 93

1 Chapter 1: Introduction

1.1 Thesis objectives and outline

The shallow portion of the subduction zone interface, the so-called “megathrust” (Lay et al. 2012), generated the largest ever recorded earthquakes, such as the 1960 Valdivia earthquake in Chile (Lorenzo-Martín, Roth, and Wang 2006; Luo et al. 2020), 2004 Sumatra earthquake in Indonesia (Chlieh et al. 2007; Subarya et al. 2006), and 2011 Tohoku-Oki earthquake in Japan (Loveless and Meade 2011; Simons et al. 2011) on the Earth. At the same time, many of the subduction zone host high populations in their coastal regions. Apart from the risk of volcanic eruptions, the subduction-related hazards put the population at a risky position in three direct and indirect ways through megathrust earthquakes, tsunami, and upper plate fault earthquakes (e.g., 1995 Kobe earthquake in Japan and 2010 Pichilemu earthquakes in Chile). This attribute of the megathrusts, along with their location offshore, raises challenges and has made them become the most difficult seismically active zone to be studied.

To solve the multifaceted behavior of the subduction zones seismic cycles at different timescale, a considerable amount of valued seismological (Schurr et al. 2014; Sippl et al. 2018), geodetical (Bedford et al. 2020; Chlieh et al. 2008; Moreno, Rosenau, and Oncken 2010), geological (Saillard et al. 2017), analog modeling (Caniven and Dominguez 2021; Corbi et al. 2013; Kosari et al. 2020; Rosenau, Corbi, and Dominguez 2017a), and numerical studies (Dinther et al. 2013; Menant et al. 2020; Wang et al. 2018, 2019) as an independent or integrated approach have been done, and many are still in progress on these highly active tectonic setting. High temporal and spatial resolution surface displacement observations have been provided for earthquake scientists thanks to Radar and GPS technology. However, they only contribute to the study of coseismic/postseismic and a fraction of the interseismic interval of a single seismic cycle (Avouac 2015). Investigating such data reveals how the coastal region goes under strain and how vertical deformation patterns look (Figure 1) (Hoffmann et al. 2018; Klein et al. 2017; Motagh et al. 2010) and slip (coseismic and slow slip) and short-term locking of the interface have been inferred (Jolivet et al. 2020). However, the remote-sensing data predominantly cover the onshore part of the upper plate in the subduction zone. The distance from the coastline to trench varies from tens of kilometers to hundreds of kilometers in different subduction zone as its average exceeds 100 km (Figure 2). In most cases, these distances are equivalent to the gap of near-source observations.

The insufficient offshore observation and the interseismic data incompleteness led earthquake scientists to employ analog and numerical modeling approaches to unfold the linkage between short-term elastic (i.e., coseismic) and long-term permanent (i.e., several seismic cycles) deformation of the subduction zones. Revealing these relationships allows us to identify which long and short-term signals earthquake scientists should look for remotely or in the field to unwrap the history of the subduction zone's seismic cycle; hence, “the past is the key to the future”.

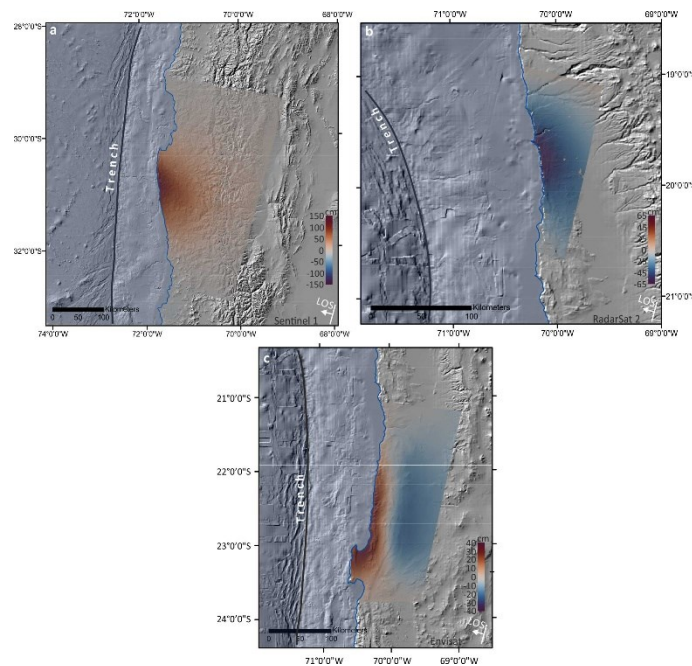


Figure 1- 1: Coseismic and early-postseismic surface deformation pattern in the direction of the line of sight derived from different large earthquakes in the Chilean subduction zone: a) Sentinel-1 unwrapped interferogram of the 2015 Illapel earthquake (Mw 8.3). b) Radarsat2 unwrapped interferogram of the Iquique 2014 earthquake (Mw 8.2 (Hoffmann et al. 2018)). c) Envisat unwrapped interferogram of the 2007 Tocopilla earthquake (Mw 7.8) (Motagh et al. 2010).

Since not much direct data are available from the shallow portion of the subduction interface, which is mainly offshore, exploring forearc reactions in terms of stress build-up and stress drop may provide a clue as to what is going on at depth. If the assumption is factual that the megathrust interface and the overlaying wedge (i.e., forearc) are mechanically coupled, any variation in interface's friction and mechanical state may be traceable as changes in the (surface) deformation pattern of the forearc.

In this study, I investigate a generic, simplified analog model of a subduction zone from trench to the location of volcanic arc and 240 km along strike using elastoplastic granular material and stick-slip analog material at a laboratory scale. The laboratory analog experiments enable us to

generate hundreds of megathrust seismic cycles and monitor the earthquake-related surface and cross-sectional deformation pattern at high resolution in both space and time. Data reduction (in coverage, density, resolution, dimension) allows us to study the effect of incomplete data, e.g., limited coverage or different temporal and spatial resolutions. I attempt to demonstrate that what surface deformation signals the frictional and mechanical changes on the interface generates over coseismic and early postseismic stages, and interseismic intervals, both elastically and permanently. This provides key observations for earthquake geoscientists to tie forearc surface deformation to subsurface elastoplastic processes at the shallow portion of the subduction interface.

Here I propose a few crucial challenges on the short- and long-term deformation of the subduction zones and try to address them by designing and running appropriate analog models: In chapter 2, I study how insufficient near-source observations may affect the inference of megathrust slip distribution and eventually bias our interpretations. In chapter 3, I show how the forearc reacts to a full stress-drop on the interface during the early postseismic phase. In chapter 3, finally, I focus on longer timescales, from tens to hundreds of megathrust earthquake cycles, and study what surface strain pattern in the forearc from trench to the coastal region can be preserved. To what extent are the strain states in the different segments of forearc similar? Furthermore, can the behavior of the offshore segment of the forearc be interpreted via onshore-limited surface observations?

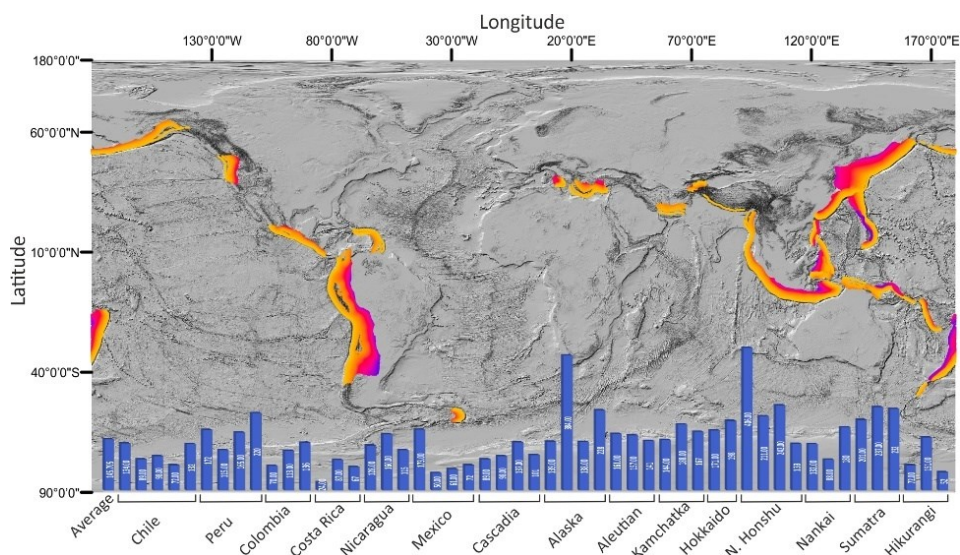


Figure 1- 2: Location of the subduction zones and their geometry (Hayes et al. 2018) and the distance from trench to the coastline (blue bar charts) in different subduction zones (Malatesta et al. 2021).

Chapters 2-4 of this dissertation are published or under-review research articles. Finally, in the fifth chapter, the key results of this research and remind steps for further research have been summarized.

1.2 Plate tectonic concept

Plate tectonics is a unifying concept that discusses the deformation patterns in the crust, distribution of earthquakes, continental drift, and seafloor spreading. This concept explains the mechanisms by which the crust and mantle of the Earth have evolved and shows that the lithosphere (the outermost layer of the Earth), behaves as a relatively rigid substance resting on a weaker layer in the mantle (i.e., asthenosphere). Additionally, this model proposed that the lithosphere consists of multiple plates that move with respect to one another while they are changing in shape and size moderately but constantly.

The plates move against and/or towards each other while moving in different speeds and various directions defined by their rotation (Euler) poles on the spherical Earth. These plate motions cause three different types of plate boundaries, including constructive, destructive, and conservative. Constructive plate boundaries are characterized by diverging plates. This divergent margin forms a gap along the separation region which is immediately filled by basaltic melts generated from the uprising mantle asthenosphere and thus generates (constructs) new crust. The divergent margins are represented by the mid-ocean ridges (i.e., seafloor mountain belts). Conservative plate boundaries occur where two plates touch each other and slide past each other. These boundaries are characterized by strike-slip or transform faulting and are commonly called transform fault plate margins. Destructive plate boundaries are characterized by converging plates where two plates move towards each other. They can be either collisional if two continental plates meet or subduction zones where oceanic and continental (or another oceanic) plates meet. In the latter case, at the meeting point of the two plates, the denser plate is pulled beneath (subducted), the less dense plate, and eventually goes down into the depths of the mantle and melts. These margins are known as “subduction zones”. From a global perspective, the drifting apart of the plates at constructive margins must be compensated by the opposite movement and destruction of the lithosphere at destructive boundaries (Frisch, Meschede, and Blakey 2010; Kearey, Klepeis, and Vine 2009).

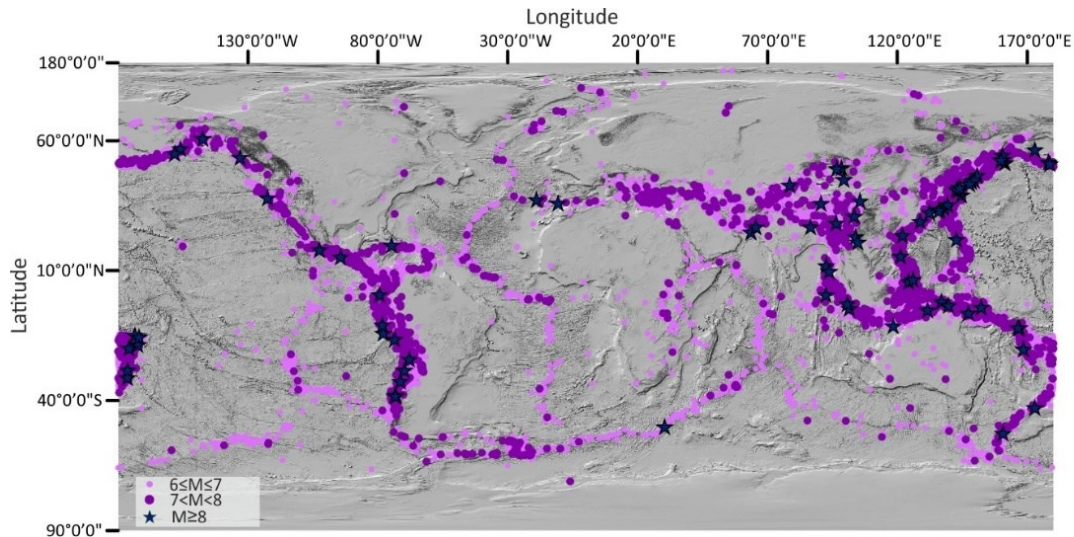


Figure 1- 3: Earth seismicity map. *The epicenter of the earthquakes with magnitudes equal and larger than 6 in the period from 1900 to 2021 is overlaid on the world SRTM30 digital elevation model. Note that majority of the large earthquakes are concentrated in the subduction zones.*

1.3 Earthquakes in subduction zones

Subduction zones are characterized by intense earthquake activity and are responsible for 95 % of all earthquakes on Earth (Figure 3). One of the features that makes these areas unique is that subductions host earthquakes with three different depth ranges: (1) shallow earthquakes, earthquakes with epicenters from near the surface to depths of 70–100 km; (2) intermediate earthquakes with depths between 70 and 400 km; and (3) deep earthquakes with depths between 350 and 700 km (Figure 4). Maximum stress is accumulated at the plate interface, where the subducting plate and the overriding plate interact by dragging, pushing, and pulling forces (Turcotte and Schubert 2002). These forces are induced by coupling of the two plates being locked at a depth range of 0 to 70 km controlled by pressure-temperature conditions (Oleskevich, Hyndman, and Wang 1999; Syracuse et al. 2010). Below this depth range, thermal conditions allow stable sliding through crystal plastic (ductile, viscous) processes of the two plates, and stress accumulation decreases to a minimum.

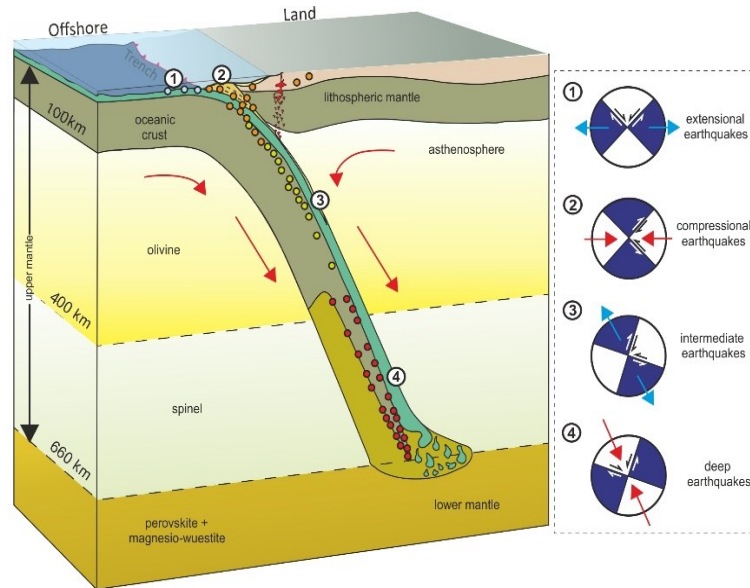


Figure 1- 4: Cross-section of a subduction zone showing the different types of earthquake mechanisms. The shallow extensional earthquakes occur in the outer-rise in the subducting plate. The uppermost area of the interface is dominated by shallow megathrust earthquakes caused by horizontal compression. Dewatering causes intermediate earthquakes to depths of 400 km. Deep earthquakes are probably created by the mineral phase transition in depths between 350 and 700 km (Frisch et al. 2010; Green 1994).

The mechanisms of earthquakes in subduction zones may also be different. The bending zone of the subducting plate, known as outer rise, is characterized by shallow normal faulting earthquakes caused by horizontal tensional stress in accordance with the formation of extensional structures (e.g., grabens). The Shallow earthquakes along the subduction zone are generated by horizontal compression and the friction between the two converging plates. The largest earthquakes on the Earth (e.g., Japan in 1923, Kamchatka in 1952, Chile in 1960, Alaska in 1964, Sumatra in 2004, Japan in 2011) occur within this zone and represent thrust mechanism. In this type of earthquake, which are known as megathrust events, the downgoing plates subduct with a rate of a few centimeters per year at a shallow angle beneath the overlying continental crust. The occurrence of large earthquakes in intervals of several decades to centuries demonstrates that the movement in the zone of friction between the two plates occurs in an apparent irregular way. Shallow thrust mechanism earthquakes in subduction zones can cause two types of devastation that can threaten coastal areas through earthquake shaking and tsunami generation (e.g., Japan 2011 and Sumatra 2004 tsunamis). The internal stress within the slab (i.e., subduction plate) generates the deepest earthquakes in subduction zones.

Intermediate and deep earthquakes are mostly tensional and compressional, respectively, while these two active zones show a gap of low seismic activity in between. The dense lithosphere of the ongoing plate sinks into the asthenosphere because of its higher density. This leads to downward-directed tensional stress within the plate and tension-caused earthquakes.

1.4 Megathrust seismic cycle

The earthquake "cycle" refers to the observation that earthquakes repeatedly (in a time span of 100 years) rupture a segment/segments of a given fault. An earthquake cycle can be decomposed into different phases, including interseismic, coseismic rupture, and postseismic phases (Figure). Our understanding of the earthquake cycle progressively grows while it leads to improving our models as well. Below four main earthquake cycle models have been summarized:

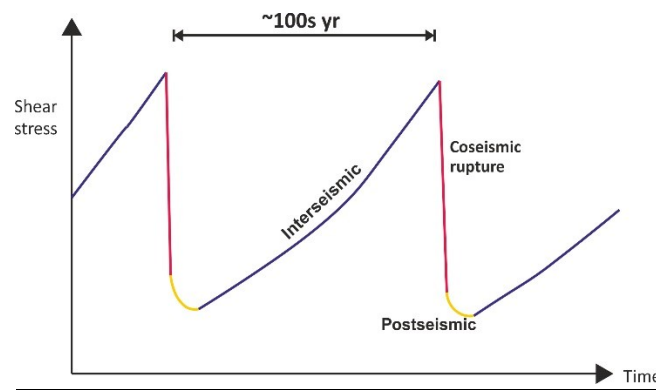


Figure 1- 5: Simplified overview of different phases of an earthquake cycle (Hicks 2015).

Periodic model: the frictional strength, the stress changes following the earthquake (i.e., stress drop), and slip on the fault are constant from event to event. It means that the timing of an earthquake and its magnitude are predictable. *Timepredictable model:* earthquakes occur when stress level reaches a threshold, but the amount of stress drop and the magnitude of slip may vary from one earthquake to another. If the strain rate of the interseismic phase is constant and that the magnitude of slip from the latest earthquake is known, this model predicts the timing of the next earthquake. However, the slip magnitude of that next earthquake is not predictable. *Slip-predictable model:* Displacement on a fault (slip) during earthquake arrests when the stress level drops to a critical level, but the stress level and strain accumulation at the time of rupture may vary between earthquakes. The model suggests that in the case of a constant interseismic strain accumulation rate, knowledge of the time since the latest earthquake, the magnitude of slip of the next earthquake is predictable. The *clustered-slip model:* In this model, also called

the “Wallace type” model, a cascade of earthquakes may occur in temporal clusters. When a cluster initiates is unpredictable, but whenever an earthquake does occur, the likelihood of another earthquake occurring afterward is high (Burbank and Anderson 2011).

Subduction zone megathrust faults host Earth’s largest earthquakes while generated about 90% of the Earth’s seismic moment in the 20th Century. This is released by devastating seismic events such as the largest ever recorded earthquakes: The Mw 9.5 Chile event in 1960, the Mw 9.2 Alaska event in 1964, and Tohoku-Oki event in 2011 (Lay et al. 2011; Lay and Bilek 2007; Pacheco and Sykes 1992) along with multitudes of smaller events that accommodate plate convergence. Sliding from the trench to the downdip transition to ductile deformation is accommodated by a combination of rapid earthquakes (small to large earthquakes), slow-slip events, and quasi-static creep (Figure 6).

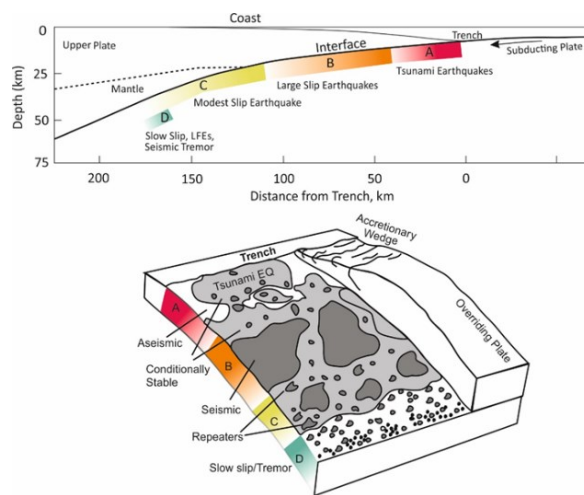


Figure 1- 6: A: Near-trench domain where tsunami earthquakes or anelastic deformation and stable sliding occur; B: Central megathrust domain where large slip occurs with minor short-period seismic radiation; C: Downdip domain where moderate slip occurs with significant coherent short-period seismic radiation; D: Transitional domain where slow slip events, low-frequency earthquakes (LFEs), and seismic tremor can occur (Lay et al. 2012).

The analysis of geodetic data at different timescales from megathrust events led to a generalized model of the deformation cycle at subduction zones. This model generally corresponds to the elastic rebound theory (Reid, 1910) and includes three main phases: (1) interseismic strain accumulation, (2) fast coseismic stress release, and (3) transient postseismic relaxation (Figures 7 and 8) (Wang, Hu, and He 2012a). (1) The interseismic phase, known as the longest phase of the seismic cycle, is the period between two earthquakes that can last decades to centuries at

subduction zones. This period is characterized by a steady accumulation of elastic strain caused by frictional stresses across the locked plate interface. The interface locking pattern is not distributed uniformly and might vary in time (Aki 1979; Moreno et al. 2011). The current locking state and a potential slip deficit of the subduction interface can be determined by analyzing ground deformation data. Recent studies showed that viscoelastic processes of the asthenosphere could relax a small portion of the interseismic stress build-up by interface locking, and this process should be considered when assessing slip deficit in relation to the seismic hazard (Wang et al. 2012a). Assessing future hazard potential posed by large earthquakes and related tsunami is the primary goal of studying the interseismic phase. Evaluating interseismic phase includes GPS measurements (Moreno et al. 2010), coastal long-term and short-term vertical movement (Saillard et al. 2017; Savage 1995), and satellite geodesy (Chlieh et al. 2004).

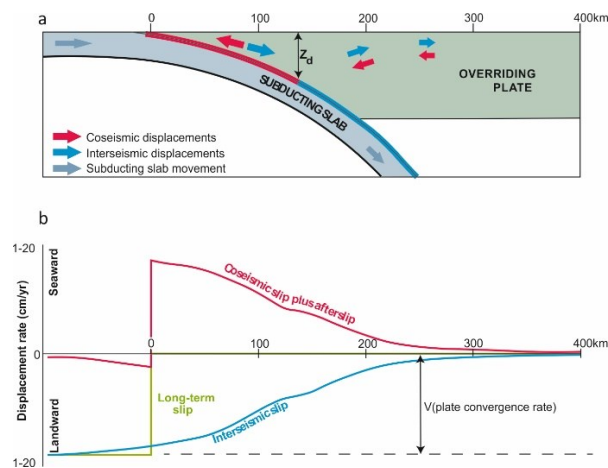


Figure 1- 7: Simplified seismic cycle on a subduction zone. Displacements at depth, indicated by red arrows (coseismic) and blue arrows (cumulated over the interseismic period). The shallower portion of the megathrust, highlighted in red, slips only during transient slip events (interplate earthquakes, afterslip, or slow slip events) and is fully locked during the interseismic period. b: Displacements at the surface: The red line represents the surface displacement rate relative to the stable overriding plate. The blue line represents the long-term surface displacement rate. The difference between the two curves, depicted by the light green line, represents the contribution of transient slip events (Avouac 2015).

(2) The interseismic phase terminates with the occurrence of a large earthquake, i.e. the coseismic phase. The shallow seismogenic part of the subduction plate interface is characterized

by velocity-weakening behavior, which leads to unstable earthquake slips (Marone 1998; Christopher H. Scholz 1998) (Figures 6 and 7). A fast (seconds to minutes) failure occurs on the plate coupling due to frictional instability of the fault interface when a stress level reaches a threshold and releases (mostly) elastic stress (Kanamori 1986). The large magnitude megathrust events transfer stress and may affect the adjacent patches to the rupture hypocenter area. This consequently leads to large aftershocks (Perfettini and Avouac 2004; Tilmann et al. 2016).

(3) The postseismic phase directly follows the coseismic phase while lasting months to years. This phase is mainly time-dependent and decays in a similar way to rheological laws (Lange et al., 2014). The phase is characterized by transient ground deformation decaying with time and involving various processes such as afterslip, viscoelastic relaxation, and relocking (Marone, Scholtz, and Bilham 1991; Wang et al. 2012a). The amount of postseismic deformation and energy release has been shown to be equal to the coseismic event (Heki, Miyazaki, and Tsuji 1997). The separation of the recorded postseismic surface deformation signal into single components requires prior assumptions about individual Spatio-temporal characteristics of each process. Near-field and relatively short-wavelength postseismic data are dominated by elastoplastic afterslip and poroelastic processes. Far-field observations show long-wavelength deformation patterns that are interpreted as induced by viscoelastic mantle relaxation extending the traditional elastic rebound theory (Kanamori 1973; Wang et al. 2012a).

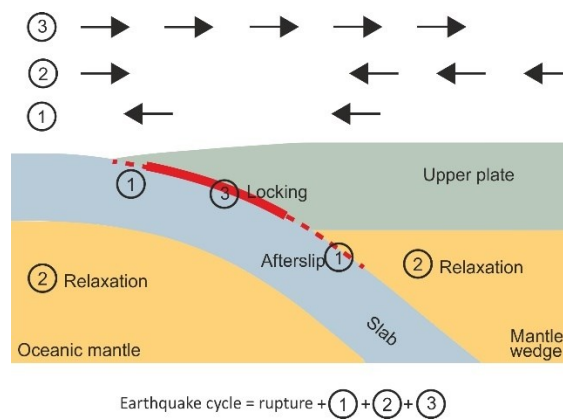


Figure 1- 8: Primary processes after a subduction earthquake. 1) Aseismic afterslip around the rupture zone, (2) viscoelastic relaxation, and (3) relocking (Wang, Hu, and He 2012b).

1.5 Experimental approaches overview

Analog earthquake modeling is one of the approaches to probe the physics of earthquakes, seismic-cycle dynamics, and seismotectonic evolution and mimic different seismically active

tectonic settings. They can be generally be categorized into three groups with increasing realism and applicability (Figure 9) (Rosenau, Corbi, and Dominguez 2017b): 1) Spring-slider model: In this model, elastic and frictional elements are physically discrete components while it can be applied conceptually to Nature. Burridge and Knopoff (1967) established the concept of a chain of coupled spring-slider systems being able to mimic earthquake occurrence and mechanisms realistically, and their results highly impacted statistical seismology. 2) Fault block models: In this model, two elastic blocks are in frictional contact. The blocks may have the same or different elastic properties. Observations from these models can be qualitatively extrapolated to Nature. 3) Seismotectonic scale models: In this model, a tectonic setting is realistically simulated on a small scale and with boundary conditions mimicking the natural prototype. These models can be directly and often quantitatively upscaled to Nature (Rosenau et al. 2017b).

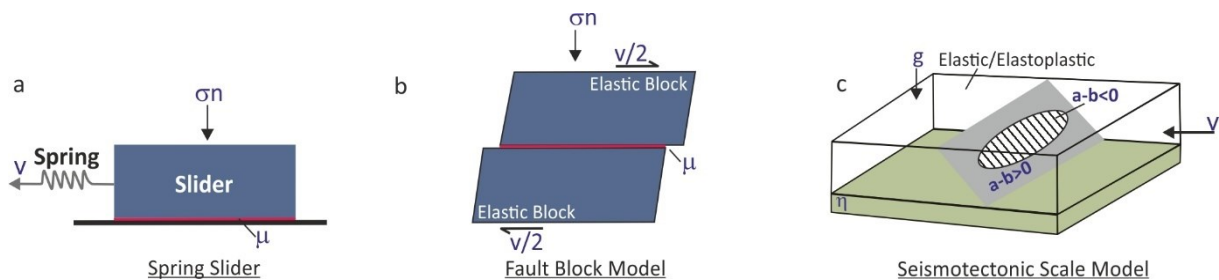


Figure 1- 9: Different types of experimental analog models: a) spring-slider model (v is velocity, σn is normal load, and μ is friction coefficient); b) fault block model; c) seismotectonic scale model ($a-b$ is rate–state parameter, η is viscosity, g is gravitational acceleration, and V is force (Rosenau et al. 2017b).

1.6 Model Scaling and similarity

The small-scale laboratory models should share geometric, kinematic, and dynamic similarities with their prototype to be representative of a natural system as all lengths, time, and forces scale down from the prototype in a consistent way dictated by scaling laws (King Hubbert 1937). According to Rosenau et al. (2009), I consider different timescales for coseismic and interseismic deformation phases. They introduced a “dyadic” timescale that recognizes two dynamically distinct regimes of the seismic cycle: the quasi-static interseismic regime, where inertial effects are negligible due to the slow deformation rates, and the dynamic coseismic regime, which is controlled by inertial effects. This allows us to slow down the earthquake rupture and speed up the loading phase, keeping dynamic similarity in both stages.

1.6.1 Interseismic phase scaling

In the quasi-static regime of the inter-seismic phase, scaling is identical to the common scaling of long-term processes to the lab. For long-term tectonic studies involving materials that deform brittle or viscous material, two dimensionless numbers, the Smoluchowski and Ramberg numbers, are of interest according to the deformation regime.

The Smoluchowski number is used to establish dynamic similarity in the case of brittle deformation. This dimensionless number is defined as the ratio between overburden stress and material strength.

$$Sm = \frac{\rho g l}{C}$$

where ρ is density (kgm^{-3}), g gravitational acceleration (ms^{-2}), C cohesion (Pa), and l a characteristic length, the Ramberg number (Ramberg, 1967) is commonly used to ensure viscous deformation similarity.

$$Ra = \frac{\rho g l}{\eta v / l}$$

where η is viscosity (Pas) and v a characteristic velocity (Ramberg, 1967).

According to Smoluchowski number, cohesion should scale according to the density and length scale following the scaling law:

$$C^* = \rho^* L^*.$$

where the asterisks represent the model / prototype ratios (i.e., $C^* = C \text{ model} / C \text{ prototype}$, $\rho^* = \rho \text{ model} / \rho \text{ prototype}$, $L^* = L \text{ model} / L \text{ prototype}$). All quantities with the stress unit (e.g., strengths) and elastic moduli share the same scaling.

Table 1: Dimensionless numbers used in analog earthquake models (Rosenau et al. 2017b).

Regime	Number	Equation	Meaning
Quasi-static	Smoluchowski	$Sm = \rho g l / C$	Gravitational-stress–brittle-strength relation
	Ramberg	$Ra = \rho g l / (\eta v / l)$	Gravitational-stress–viscous-strength relation
	Stokes	$St = \Delta P / (\eta v / l)$	Pressure–viscosity relation
Dynamic	Reynolds	$Re = \rho v l / \eta$	Inertia–viscosity relation
	Froude	$Fr = v / (g l)^{1/2}$	Inertia–gravity relation
	Cauchy	$Ca = \rho v^2 / B$	Inertia–elasticity

1.6.2 Coseismic phase scaling

For a short-term time (i.e., coseismic and postseismic stages), Froude scaling is used to reach dynamic similarity (Rosenau et al., 2009):

$$Fr = v / \sqrt{gl} = \text{inertia / gravitation}$$

while the timescale of the model should be the square root of the length scale:

$$T^* = \sqrt{L^*}$$

Note that all accelerations are the same in the model as in the prototype. The Cauchy number can be used for reaching the stress scale in the dynamic regime (Rosenau, Lohrmann, and Oncken 2009b):

$$Ca = \rho v^2 / B = \text{inertia/elasticity}$$

where B is an elastic modulus.

The model parameters without a dimension should be preserved Poisson's ratio ν , the friction coefficient, the friction rate and state parameters. An exception to this general scale independence of dimensionless parameters is the moment magnitude M_w that is related to the seismic moment (unit Nm) but defined as being dimensionless:

$$M_w = 2/3 \log_{10} (M_0) - 10.7$$

Here I scale up analog earthquake moment magnitude non-linearly by applying the scale factor of seismic moment M_0^* :

$$M_w^{\text{prototype}} = M_w^{\text{model}} - 2/3 \log M_0^*$$

Typically, magnitudes of analog earthquakes are in the range of -6 to -7 , which correspond to earthquakes of $M_w = 8-9$ in Nature.

Table 2: Typical scales, scaling relations, and factors in seismotectonic scale models (Rosenau et al. 2019).

Model Parameters and Scaling Relations										
Parameters										
	Quantity	Dimension {M,L,T}		Unit	Model		Nature		Dimensionless number	Scaling factor
Model geometry and kinematics	Length Seismic	l	D	L	[m]	1	cm	3	km	$3.3 \cdot 10^{-6}$
	slip Recurrence	T_{rec}		L	[m]	100	μm	30	m	$3.3 \cdot 10^{-6}$
	time Rupture	T_{rup}		T	[s]	4	s	1000	a	$1.3 \cdot 10^{-10}$
	duration	v		T	[s]	<0.1	s	<1	min	$1.8 \cdot 10^{-3}$
	Convergence	v'		L/T	[m/s]	50	$\mu\text{m/s}$	60	mm/a	$2.6 \cdot 10^4$
	velocity Rupture	g		L/T	[m/s]	5	m/s	3	km/s	$1.8 \cdot 10^{-3}$
	velocity			L/T ²	[m/s ²]	9.81	m/s ²	9.81	m/s ²	1
Coseismic acceleration	a'		L/T ²	[m/s ²]	0.6	m/s ²	0.6	m/s ²	1	
Material properties	Friction coefficient ^a	μ				0.7		0.7		1
	Friction rate parameter	a-b				+/-0.02		+/-0.02		1
	Cohesion	C	E	M/LT ²	[Pa]	10		100	MPa	$1.1 \cdot 10^{-6}$
	Young's modulus	η		M/LT ²	[Pa]	100		100	GPa	$1.1 \cdot 10^{-6}$
	Viscosity	ρ		M/LT	[Pas]	$2 \cdot 10^4$		10^{20}	Pas	$1.4 \cdot 10^{-16}$
Density	G		M/L ³	[kg/m ³]	900	kg/m ³	2800	kg/m ³	$3.3 \cdot 10^{-1}$	
Forces	Gravitation	I		ML/T ²	[N]					$1.2 \cdot 10^{-17}$
	Inertia	τ		ML/T ²	[N]					$1.2 \cdot 10^{-17}$
Strength & energy	Strength ^b	$\Delta\tau$		M/LT ²	[Pa]	500	Pa	500	MPa	$1.1 \cdot 10^{-6}$
	Stress drop	M_0		M/LT ²	[Pa]	100	Pa	100	MPa	$1.1 \cdot 10^{-6}$
	Seismic moment			ML ² /T ²	[Nm]	1	Nm	$3 \cdot 10^{22}$	Nm	$4.0 \cdot 10^{-23}$

Note. M = Mass; L = Length; T = Time.
^aInterseismic. ^bAt seismogenic depth.

1.7 The Rate-and-State Framework

In a simple picture, the shear stress τ along a planar surface is directly proportional to the normal stress σN acting upon it. With the linear friction coefficient μ :

$$\tau = \mu \sigma N$$

Although a Coulomb friction model is assumed for brittle failure with a constant coefficient of friction, for systems that switch from stationary (interseismic) to unstable mode (coseismic), two different static and dynamic frictions have been established (Rabinowicz 1951, 1956). The static friction (μ_s) holds the two sides of a fault immobile, called the static friction, and that friction becomes dynamic (μ_d) as the two sides of the fault grind past one another while evolving throughout an earthquake.

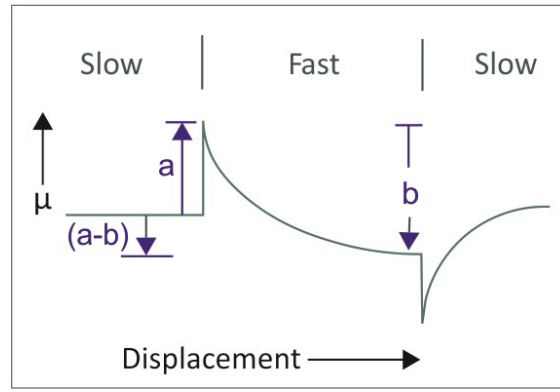


Figure 1-10: Schematic diagram defining the terms in the rate–state friction law (C. H. Scholz 1998).

The behavior of frictional is commonly defined in the framework of rate-and-state friction (RSF) (Scholz 2018). The framework describes relations between the coefficient of friction (μ), rate of deformation (V), and “state” (θ):

$$\mu(V, \theta) = \mu^* + a \ln\left(\frac{V}{V^*}\right) + b \ln\left(\frac{V^* \theta}{Dc}\right)$$

where μ^* is the coefficient of friction measured at sliding velocity V^* . The parameters a and b represent the frictional properties of the material. The parameter $(a - b)$ represents the velocity-dependence of μ at steady-state, with positive values (i.e. $a > b$) resulting in velocity-strengthening and negative values resulting in velocity-weakening behavior (seismogenic zone) (Figures 10 and 11). The characteristic slip distance Dc controls the slip distance over which the evolution towards the new steady-state takes place. The evolution of the state parameter θ is formulated either by the “ageing law” (Dieterich 1979) or “slip law” (Ruina 1983):

$$\frac{d\theta}{dt} = 1 - \frac{V\theta}{Dc}$$

$$\frac{d\theta}{dt} = -\frac{V\theta}{Dc} \ln\left(\frac{V\theta}{Dc}\right)$$

The data from slide–hold–slide experiments demonstrate the effects of time and velocity on friction. The steady-state sliding follows by a quasi-static holding for a hold time (t), followed by a resumption of slip at the same slip velocity as before. An increase of friction ($\Delta\mu_s$) is clear concurrent with initiation of sliding and followed by a decay to the previous value before sliding. The static friction (μ_s) increases with hold time. The data from the velocity stepping test shows that the slip velocity is abruptly increased by order of magnitude. The dynamic friction (μ_d) depends on sliding velocity.

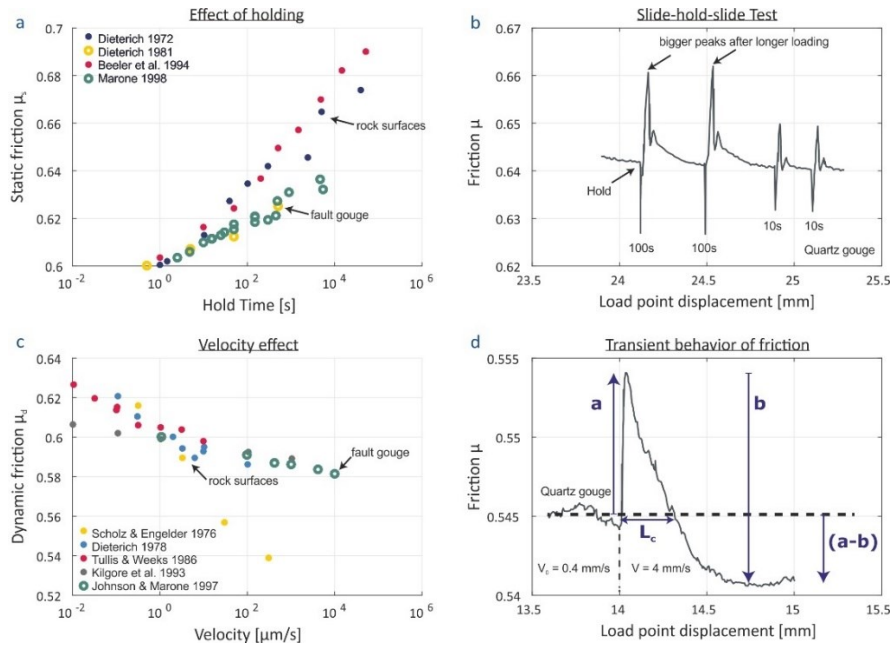


Figure 1- 11: Experimental results from slide-hold-slide tests (Marone 1998). (A): The strength of the fault zone increases with increasing hold time. (B): Typical curve of a slide-hold-slide test showing reloading peaks after 100 s and 10 s. (C): The velocity weakening behavior of fault gouges and rock surfaces. (D): Evolution of friction during a velocity stepping test (Rudolf 2019).

1.8 Analog materials and experimental setup

The experimental setup is modified from the 3-D setup used in Rosenau et al. (2019). The subduction forearc model wedge is set up in a glass-sided box (1,000 mm across strike, 800 mm along strike, and 300mmdeep) with a dipping, elastic basal conveyor belt and a rigid backwall. The analog subduction zone models consist of an elastic-frictional plastic (elastoplastic) continental lithosphere made of granular material composed of mixtures of rice, salt, rubber powder. Frictional properties of granular experimental materials, such as cohesion (C), internal friction coefficient (μ), friction rate parameter ($a-b$) have been measured using a Schulze ring shear tester. I performed velocity stepping tests at variable normal load and variable shear rate. The elasticity of experimental materials has been measured using a uniaxial compression tester. The material tests and the experiments have been run at constant temperature (23°C) and dry room climate (30–40% humidity).

Zones of velocity weakening controlled stick-slip (“seismic” behavior) are realized by emplacing compartments of either rice (“main slip patches”) or fine salt grain (“matrix”), which generate quasi-periodic large and small slip instabilities, respectively, mimicking megathrust earthquakes of different size and frequency. Large stick-slip instabilities in the main slip

patch(es) (MSP) are almost complete and recur at low frequency (~ 0.2 Hz), while those in the matrix are partial. Slip surfaces developed in the rice and salt show a remarkably regular stick-slip pattern resulting in a sawtooth-like time-stress curve while increasing the normal load causes a longer recurrence interval and a larger stress drop. The main “coseismic” deformation mechanism is particle boundary sliding. A wedge made of an elastoplastic sand- rubber mixture (50 vol.% quartz sand G12: 50 vol.% EPDM-rubber) to yield desired elastic effects and sieved into the setup representing a 240 km long forearc segment from the trench to the volcanic arc. The wedge responds elastically to these basal slip events similar to crustal rebound during natural subduction megathrust earthquakes.

1.8.1 Laboratory geodesy

To capture horizontal micrometer-scale surface displacements associated with analog earthquakes at microsecond scale periods, I monitor the model surface with different digital cameras depending on the required spatial and temporal resolution. Spatial and temporal resolutions usually represent a negative correlation, as a high spatial resolution can be achieved with a lower temporal resolution. Digital image correlation (Adam et al. 2005) has been applied via the DAVIS 8 and 10 software (LaVision GmbH, Göttingen/DE). Data are processed to yield observational data similar to those from an ideal dense and full coverage (on and offshore) geodetic network, that is, velocities (or incremental displacements) at locations on the model surface. I use an analog geodetic slip inversion technique to invert surface displacements for model megathrust slip and backslip distribution over earthquake cycles. The cameras properties used for monitoring the experiments are summarized as:

Table 3: List of cameras that are used for the experiment monitoring.

CAMERA MODEL	SPATIAL RESOLUTION [PX]	MAX. FRAMERATE [HZ]	BIT DEPTH [BIT]
IMAGER PROX 11M	4008×2672	5	16
PHANTOM VEO-640L	2560×1600	1400	10
IMAGER MX4M	2048×2048	37 - 185	8-12

1.8.2 Inversion Procedure

I use the analog geodetic slip inversion technique (Chapter 2), which estimates slip distribution from surface displacement observations in a customized fashion tailored to analog earthquakes. All three components of the static coseismic surface displacement vectors derived from DIC are used as input data for the inversion procedure. For the inversion, the full model megathrust interface, including seismogenic and aseismic areas, is discretized by evenly sized dislocations.

I tackle the inverse problem using damped bound-constrained least squares (DBCLS), and the problem is designed and solved based on convex optimization (Boyd and Vandenberghe 2004). To tie coseismic slip in individual fault patches to the observed surface displacement vectors at individual surface points, Green's functions for rectangular dislocations in an elastic half-space (Okada 1985) are computed and applied, and the dip-slip vector is solved for each patch. The Green's functions change from each analog earthquake to another to account for subtle geometric changes of the model wedge (mainly trench position) over multiple seismic cycles. I use a Laplacian regularization to stabilize the inverse problem and produce a more physically feasible slip inversion model (Kositsky and Avouac 2010).

1.9 References:

- Adam, J., J. L. Urai, B. Wieneke, O. Oncken, K. Pfeiffer, N. Kukowski, J. Lohrmann, S. Hoth, W. Van Der Zee, and J. Schmatz. 2005. "Shear Localisation and Strain Distribution during Tectonic Faulting—New Insights from Granular-Flow Experiments and High-Resolution Optical Image Correlation Techniques." *Journal of Structural Geology* 27(2):283–301.
- Aki, Keiiti. 1979. "Characterization of Barriers on an Earthquake Fault." *Journal of Geophysical Research: Solid Earth* 84(B11):6140–48.
- Avouac, Jean-Philippe. 2015. "From Geodetic Imaging of Seismic and Aseismic Fault Slip to Dynamic Modeling of the Seismic Cycle." *Annual Review of Earth and Planetary Sciences* 43(1):233–71.
- Bedford, Jonathan R., Marcos Moreno, Zhiguo Deng, Onno Oncken, Bernd Schurr, Timm John, Juan Carlos Báez, and Michael Bevis. 2020. "Months-Long Thousand-Kilometre-Scale Wobbling before Great Subduction Earthquakes." *Nature* 2020 580:7805 580(7805):628–35.
- Boyd, Stephen and Lieven Vandenbergh. 2004. *Convex Optimization*. Cambridge university press.
- Burbank, Douglas W. and Robert S. Anderson. 2011. *Tectonic Geomorphology*. John Wiley & Sons.
- Caniven, Yannick and Stéphane Dominguez. 2021. "Validation of a Multilayered Analog Model Integrating Crust-Mantle Visco-Elastic Coupling to Investigate Subduction Megathrust Earthquake Cycle." *Journal of Geophysical Research: Solid Earth* 126(2):e2020JB020342.
- Chlieh, M., J. P. Avouac, K. Sieh, D. H. Natawidjaja, and John Galetzka. 2008. "Heterogeneous Coupling of the Sumatran Megathrust Constrained by Geodetic and Paleogeodetic Measurements." *Journal of Geophysical Research: Solid Earth* 113(5).
- Chlieh, M., J. B. De Chabalier, J. C. Ruegg, R. Armijo, R. Dmowska, J. Campos, and K. L. Feigl. 2004. "Crustal Deformation and Fault Slip during the Seismic Cycle in the North Chile Subduction Zone, from GPS and InSAR Observations." *Geophysical Journal International* 158(2):695–711.
- Chlieh, Mohamed, Jean-Philippe Avouac, Vala Hjorleifsdottir, Teh-Ru Alex Song, Chen Ji,

- Kerry Sieh, Anthony Sladen, Helene Hebert, Linette Prawirodirdjo, Yehuda Bock, and John Galetzka. 2007. “Coseismic Slip and Afterslip of the Great Mw 9.15 Sumatra–Andaman Earthquake of 2004.” *Bulletin of the Seismological Society of America* 97(1A):S152–73.
- Corbi, F., F. Funiciello, M. Moroni, Y. Van Dinther, P. M. Mai, L. A. Dalguer, and C. Faccenna. 2013. “The Seismic Cycle at Subduction Thrusts: 1. Insights from Laboratory Models.” *Journal of Geophysical Research: Solid Earth* 118(4):1483–1501.
- Dieterich, James H. 1979. “Modeling of Rock Friction: 1. Experimental Results and Constitutive Equations.” *Journal of Geophysical Research: Solid Earth* 84(B5):2161–68.
- Dinther, Y. van, T. V. Gerya, L. A. Dalguer, P. M. Mai, G. Morra, and D. Giardini. 2013. “The Seismic Cycle at Subduction Thrusts: Insights from Seismo-Thermo-Mechanical Models.” *Journal of Geophysical Research: Solid Earth* 118(12):6183–6202.
- Frisch, Wolfgang, Martin Meschede, and Ronald C. Blakey. 2010. *Plate Tectonics: Continental Drift and Mountain Building*. Springer Science & Business Media.
- Green, Harry W. 1994. “Solving the Paradox of Deep Earthquakes.” *Scientific American* 271(3):64–71.
- Hayes, Gavin P., Ginevra L. Moore, Daniel E. Portner, Mike Hearne, Hanna Flamme, Maria Furtney, and Gregory M. Smoczyk. 2018. “Slab2, a Comprehensive Subduction Zone Geometry Model.” *Science* 362(6410):58–61.
- Heki, Kosuke, Shin’ichi Miyazaki, and Hiromichi Tsuji. 1997. “Silent Fault Slip Following an Interplate Thrust Earthquake at the Japan Trench.” *Nature* 1997 386:6625 386(6625):595–98.
- Hicks, Stephen Paul. 2015. “Seismic Properties and Processes along the Subduction Plate Interface: The February 2010 M w 8.8 Maule, Chile Earthquake.” University of Liverpool.
- Hoffmann, Felix, Sabrina Metzger, Marcos Moreno, Zhiguo Deng, Christian Sippl, Francisco Ortega-Culaciati, and Onno Oncken. 2018. “Characterizing Afterslip and Ground Displacement Rate Increase Following the 2014 Iquique-Pisagua Mw 8.1 Earthquake, Northern Chile.” *Journal of Geophysical Research: Solid Earth* 123(5):4171–92.
- Jolivet, R., M. Simons, Z. Duputel, J. A. Olive, H. S. Bhat, and Q. Bletery. 2020.

- “Interseismic Loading of Subduction Megathrust Drives Long-Term Uplift in Northern Chile.” *Geophysical Research Letters* 47(8):e2019GL085377.
- Kanamori, Hiroo. 1973. “Mode of Strain Release Associated with Major Earthquakes in Japan.” *Annual Review of Earth and Planetary Sciences* 1(1):213–39.
- Kanamori, Hiroo. 1986. “RUPTURE PROCESS OF SUBDUCTION-ZONE EARTHQUAKES.” *Ann. Rev. Earth Planet. Sci* 14:293–322.
- Kearey, Philip, Keith A. Klepeis, and Frederick J. Vine. 2009. *Global Tectonics*. John Wiley & Sons.
- King Hubbert, M. 1937. “Theory of Scale Models as Applied to the Study of Geologic Structures.” *Bulletin of the Geological Society of America* 48(10):1459–1520.
- Klein, E., C. Vigny, L. Fleitout, R. Grandin, R. Jolivet, E. Rivera, and M. Métois. 2017. “A Comprehensive Analysis of the Illapel 2015 Mw8.3 Earthquake from GPS and InSAR Data.” *Earth and Planetary Science Letters* 469:123–34.
- Kosari, Ehsan, Matthias Rosenau, Jonathan Bedford, Michael Rudolf, and Onno Oncken. 2020. “On the Relationship Between Offshore Geodetic Coverage and Slip Model Uncertainty: Analog Megathrust Earthquake Case Studies.” *Geophysical Research Letters* 47(15).
- Kositsky, A. P. and J. P. Avouac. 2010. “Inverting Geodetic Time Series with a Principal Component Analysis-Based Inversion Method.” *Journal of Geophysical Research: Solid Earth* 115(3).
- Lay, Thorne, Charles J. Ammon, Hiroo Kanamori, Lian Xue, and Marina J. Kim. 2011. “Possible Large Near-Trench Slip during the 2011 Mw 9.0 off the Pacific Coast of Tohoku Earthquake.” *Earth, Planets and Space* 63(7):687–92.
- Lay, Thorne and Susan Bilek. 2007. “15. Anomalous Earthquake Ruptures at Shallow Depths on Subduction Zone Megathrusts.” Pp. 476–511 in *The seismogenic zone of subduction thrust faults*. Columbia University Press.
- Lay, Thorne, Hiroo Kanamori, Charles J. Ammon, Keith D. Koper, Alexander R. Hutko, Lingling Ye, Han Yue, and Teresa M. Rushing. 2012. “Depth-Varying Rupture Properties of Subduction Zone Megathrust Faults.” *Journal of Geophysical Research: Solid Earth* 117(4).

- Lorenzo-Martín, Francisco, Frank Roth, and Rongjiang Wang. 2006. “Inversion for Rheological Parameters from Post-Seismic Surface Deformation Associated with the 1960 Valdivia Earthquake, Chile.” *Geophysical Journal International* 164(1):75–87.
- Loveless, John P. and Brendan J. Meade. 2011. “Spatial Correlation of Interseismic Coupling and Coseismic Rupture Extent of the 2011 $M_w = 9.0$ Tohoku-Oki Earthquake.” *Geophysical Research Letters* 38(17).
- Luo, Haipeng, Boudewijn Ambrosius, Raymond M. Russo, Victor Mocanu, Kelin Wang, Michael Bevis, and Rui Fernandes. 2020. “A Recent Increase in Megathrust Locking in the Southernmost Rupture Area of the Giant 1960 Chile Earthquake.” *Earth and Planetary Science Letters* 537:116200.
- Malatesta, Luca C., Lucile Bruhat, Noah J. Finnegan, and Jean-Arthur L. Olive. 2021. “Co-Location of the Downtip End of Seismic Coupling and the Continental Shelf Break.” *Journal of Geophysical Research: Solid Earth* 126(1):e2020JB019589.
- Marone, Chris. 1998. “Laboratory-Derived Friction Laws and Their Application to Seismic Faulting.” *Annual Review of Earth and Planetary Sciences* 26(1):643–96.
- Marone, Chris J., C. H. Scholtz, and Roger Bilham. 1991. “On the Mechanics of Earthquake Afterslip.” *Journal of Geophysical Research: Solid Earth* 96(B5):8441–52.
- Menant, Armel, Samuel Angiboust, Taras Gerya, Robin Lacassin, Martine Simoes, and Raphael Grandin. 2020. “Transient Stripping of Subducting Slabs Controls Periodic Forearc Uplift.” *Nature Communications* 2020 11:1 11(1):1–10.
- Moreno, M., D. Melnick, M. Rosenau, J. Bolte, J. Klotz, H. Echtler, J. Baez, K. Bataille, J. Chen, M. Bevis, H. Hase, and O. Oncken. 2011. “Heterogeneous Plate Locking in the South–Central Chile Subduction Zone: Building up the next Great Earthquake.” *Earth and Planetary Science Letters* 305(3–4):413–24.
- Moreno, Marcos, Matthias Rosenau, and Onno Oncken. 2010. “2010 Maule Earthquake Slip Correlates with Pre-Seismic Locking of Andean Subduction Zone.” *Nature* 2010 467:7312 467(7312):198–202.
- Motagh, Mahdi, Bernd Schurr, Jan Anderssohn, Beatrice Cailleau, Thomas R. Walter, Rongjiang Wang, and Jean Pierre Villotte. 2010. “Subduction Earthquake Deformation Associated with 14 November 2007, Mw 7.8 Tocopilla Earthquake in Chile: Results

- from InSAR and Aftershocks.” *Tectonophysics* 490(1–2):60–68.
- Okada, Yoshimitsu. 1985. *SURFACE DEFORMATION DUE TO SHEAR AND TENSILE FAULTS IN A HALF-SPACE*. Vol. 75.
- Oleskevich, D. A., R. D. Hyndman, and K. Wang. 1999. “The Updip and Downdip Limits to Great Subduction Earthquakes: Thermal and Structural Models of Cascadia, South Alaska, SW Japan, and Chile.” *Journal of Geophysical Research: Solid Earth* 104(B7):14965–91.
- Pacheco, Javier F. and Lynn R. Sykes. 1992. “Seismic Moment Catalog of Large Shallow Earthquakes, 1900 to 1989.” *Bulletin of the Seismological Society of America* 82(3):1306–49.
- Perfettini, H. and J. P. Avouac. 2004. “Postseismic Relaxation Driven by Brittle Creep: A Possible Mechanism to Reconcile Geodetic Measurements and the Decay Rate of Aftershocks, Application to the Chi-Chi Earthquake, Taiwan.” *Journal of Geophysical Research: Solid Earth* 109(B2):2304.
- Rabinowicz, Ernest. 1951. “The Nature of the Static and Kinetic Coefficients of Friction.” *Journal of Applied Physics* 22(11):1373–79.
- Rabinowicz, Ernest. 1956. “Stick and Slip.” *Scientific American* 194(5):109–19.
- Rosenau, Matthias, Fabio Corbi, and Stephane Dominguez. 2017a. “Analogue Earthquakes and Seismic Cycles: Experimental Modelling across Timescales. Solid Earth, European Geosciences Union.” 8(3):597–635.
- Rosenau, Matthias, Fabio Corbi, and Stephane Dominguez. 2017b. “Analogue Earthquakes and Seismic Cycles: Experimental Modelling across Timescales.” *Solid Earth* 8(3):597–635.
- Rosenau, Matthias, Illia Horenko, Fabio Corbi, Michael Rudolf, Ralf Kornhuber, and Onno Oncken. 2019. “Synchronization of Great Subduction Megathrust Earthquakes: Insights From Scale Model Analysis.” *Journal of Geophysical Research: Solid Earth* 124(4):3646–61.
- Rosenau, Matthias, Jo Lohrmann, and Onno Oncken. 2009a. “Shocks in a Box: An Analogue Model of Subduction Earthquake Cycles with Application to Seismotectonic Forearc Evolution.” *Journal of Geophysical Research: Solid Earth* 114(B1):1409.

- Rosenau, Matthias, Jo Lohrmann, and Onno Oncken. 2009b. "Shocks in a Box: An Analogue Model of Subduction Earthquake Cycles with Application to Seismotectonic Forearc Evolution." *Journal of Geophysical Research: Solid Earth* 114(1).
- Rudolf, Michael. 2019. *Velocity Dependent Rheologies in Seismotectonic Scale Modelling: Characterization and Implementation in a New Analogue Modelling Scheme*. Freie Universitaet Berlin (Germany).
- Ruina, Andy. 1983. "Slip Instability and State Variable Friction Laws." *Journal of Geophysical Research: Solid Earth* 88(B12):10359–70.
- Saillard, M., L. Audin, B. Rousset, J. P. Avouac, M. Chlieh, S. R. Hall, L. Husson, and D. L. Farber. 2017. "From the Seismic Cycle to Long-Term Deformation: Linking Seismic Coupling and Quaternary Coastal Geomorphology along the Andean Megathrust." *Tectonics* 36(2):241–56.
- Savage, J. C. 1995. "Interseismic Uplift at the Nankai Subduction Zone, Southwest Japan, 1951–1990." *Journal of Geophysical Research: Solid Earth* 100(B4):6339–50.
- Scholz, C. H. 1998. "Earthquakes and Friction Laws." *Nature* 391(6662):37–42.
- Scholz, Christopher H. 1998. "Earthquakes and Friction Laws." *Nature* 1998 391:6662 391(6662):37–42.
- Scholz, Christopher H. 2018. "The Mechanics of Earthquakes and Faulting." *The Mechanics of Earthquakes and Faulting*.
- Schurr, Bernd, Günter Asch, Sebastian Hainzl, Jonathan Bedford, Andreas Hoechner, Mauro Palo, Rongjiang Wang, Marcos Moreno, Mitja Bartsch, Yong Zhang, Onno Oncken, Frederik Tilmann, Torsten Dahm, Pia Victor, Sergio Barrientos, and Jean-Pierre Vilotte. 2014. "Gradual Unlocking of Plate Boundary Controlled Initiation of the 2014 Iquique Earthquake." *Nature* 2014 512:7514 512(7514):299–302.
- Simons, Mark, Sarah E. Minson, Anthony Sladen, Francisco Ortega, Junle Jiang, Susan E. Owen, Lingsen Meng, Jean-Paul Ampuero, Shengji Wei, Risheng Chu, Donald V. Helmberger, Hiroo Kanamori, Eric Hetland, Angelyn W. Moore, and Frank H. Webb. 2011. "The 2011 Magnitude 9.0 Tohoku-Oki Earthquake: Mosaicking the Megathrust from Seconds to Centuries." *Science* 332(6036):1421–25.
- Sippl, C., B. Schurr, G. Asch, and J. Kummerow. 2018. "Seismicity Structure of the Northern

- Chile Forearc From >100,000 Double-Difference Relocated Hypocenters.” *Journal of Geophysical Research: Solid Earth* 123(5):4063–87.
- Subarya, Cecep, Mohamed Chlieh, Linette Prawirodirdjo, Jean-Philippe Avouac, Yehuda Bock, Kerry Sieh, Aron J. Meltzner, Danny H. Natawidjaja, and Robert McCaffrey. 2006. “Plate-Boundary Deformation Associated with the Great Sumatra–Andaman Earthquake.” *Nature* 2006 440:7080 440(7080):46–51.
- Syracuse, Ellen M., Peter E. van Keken, Geoffrey A. Abers, Daisuke Suetsugu, Craig Bina, Toru Inoue, Douglas Wiens, and Mark Jellinek. 2010. “The Global Range of Subduction Zone Thermal Models.” *Physics of the Earth and Planetary Interiors* 183(1–2):73–90.
- Tilmann, F., Y. Zhang, M. Moreno, J. Saul, F. Eckelmann, M. Palo, Z. Deng, A. Babeyko, K. Chen, J. C. Baez, B. Schurr, R. Wang, and T. Dahm. 2016. “The 2015 Illapel Earthquake, Central Chile: A Type Case for a Characteristic Earthquake?” *Geophysical Research Letters* 43(2):574–83.
- Turcotte, Donald L. and Gerald Schubert. 2002. *Geodynamics*. Cambridge university press.
- Wang, Kelin, Lonn Brown, Yan Hu, Keisuke Yoshida, Jiangheng He, and Tianhaozhe Sun. 2019. “Stable Forearc Stressed by a Weak Megathrust: Mechanical and Geodynamic Implications of Stress Changes Caused by the M = 9 Tohoku-Oki Earthquake.” *Journal of Geophysical Research: Solid Earth* 124(6):6179–94.
- Wang, Kelin, Yan Hu, and Jiangheng He. 2012a. “Deformation Cycles of Subduction Earthquakes in a Viscoelastic Earth.” *Nature* 484(7394):327–32.
- Wang, Kelin, Yan Hu, and Jiangheng He. 2012b. “Deformation Cycles of Subduction Earthquakes in a Viscoelastic Earth.” *Nature* 484(7394):327–32.
- Wang, Kelin, Tianhaozhe Sun, Lonn Brown, Ryota Hino, Fumiaki Tomita, Motoyuki Kido, Takeshi Iinuma, Shuichi Kodaira, and Toshiya Fujiwara. 2018. “Learning from Crustal Deformation Associated with the M9 2011 Tohoku-Oki Earthquake.” *Geosphere* 14(2):552–71.

2 Chapter 2: On the relationship between offshore geodetic coverage and slip model uncertainty: Analog megathrust earthquake case studies

published as: Kosari et al. (2020): "On the relationship between offshore geodetic coverage and slip model uncertainty: Analog megathrust earthquake case studies." *Geophysical Research Letters* 47.15 (2020). DOI: <https://doi.org/10.1029/2020GL088266>.

All data underlying this chapter are published open access in Kosari et al. (2020) as "Digital image correlation data from analogue subduction megathrust earthquakes addressing the control of geodetic coverage on coseismic slip inversion". DOI: <https://doi.org/10.5880/GFZ.4.1.2020.003>

Individual Contributions: E. Kosari performed the research, carried out experiments, analysed results, and wrote the paper; Ma. R. participated in writing the paper and supervised the research; J.B. participated in analyzing data and improving the manuscript; Mi.R. participated in the laboratory works and improving the manuscript; O. O. was involved in planning the research, supervised the research, participated in writing the paper.

3 Chapter 3: Postseismic backslip as a response to a sequential elastic rebound of upper plate and slab in subduction zones

Under revision for Journal of Geophysical Research (JGR) and available in a preprint server as E. Kosari et al. "Postseismic backslip as a response to a sequential elastic rebound of upper plate and slab in subduction zones." Earth and Space Science Open Archive ESSOAr (2021). <https://doi.org/10.1002/essoar.10506467.1>

Individual Contributions: E. Kosari performed the research, carried out experiments, analyzed results, and wrote the paper; Ma. R. participated in writing the paper and supervised the research; Th.Z. Participated in the laboratory works and designing electronic tools; O. O. was involved in planning the research, supervised the research, and participated in writing the paper.

4 Chapter 4: Strain signals governed by frictional-elastoplastic interaction of the upper plate and shallow subduction megathrust interface over seismic cycles

Submitted to Journal of Tectonics and available in a preprint server as E. Kosari et al. "Strain signals governed by frictional- elastoplastic interaction of the upper plate and shallow subduction megathrust interface over seismic cycles." <https://doi.org/10.1002/essoar.10508266.1>

Individual Contributions: E. Kosari performed the research, carried out experiments, analyzed results, and wrote the paper; Ma. R. participated in writing the paper and supervised the research; O. O. was involved in planning the research, supervised the research participated in writing the paper.

5 Chapter 5: Conclusions and outlook

5.1 Conclusions and outlook

5.1.1 Conclusions

The key messages of my PhD thesis are summed up in the following list:

- Slip inversion models of analog earthquakes show quantitative and qualitative changes as a function of offshore geodetic coverage: For trench-breaking (A-B-type) events, changes in the slip estimations become significant when the observations cover less than 70% of the offshore distance to the trench and a significant seismic moment underestimation ($\sim M_w=0.5$), unlike for B-C type event, is suggested as coverage is reduced to $<70\%$.
- Inverted slip for trench-breaking and non-trench-breaking events converges to a similar pattern when there is no offshore geodetic coverage. I infer 5-20% slip overestimation when the observations are above the high slipping zone during trench-breaking events versus 5-10% underestimation during non-trench-breaking events if observations are land-limited.
- A sequential elastic rebound follows the coseismic shear-stress drop in the elastic-frictional models: a fast rebound of the upper plate and the delayed and smaller rebound on the slab.
- A combination of the delayed rebound of the slab and the rapid relaxation of the upper plate after an elastic overshooting may accelerate the relocking of the megathrust. This acceleration triggers/antedates the failure of a nearby asperity and enhances the early backslip in the rupture area.
- In the shallow portion of the subduction zone, frictional properties of the interface and mechanical characteristics of the forearc determine the surface deformation signal over seismic cycles. The interaction between the shallow wedge and the interface can partition the wedge into different segments. These segments may react analogously or oppositely over the different intervals of the seismic cycle. We highlight that a more segmented upper plate represents megathrust subduction that generates more characteristic and periodic events. Moreover, different wedge segments may switch their strain state from compression/extension to extension/compression domains.
- The strain time series reveal that the strain state may switch the mode after remaining quasi-stable over a few seismic cycles in the coastal zone. I show that the mechanical

state of the plate interface beneath the coastal region, may vary over time and influence the coastal region strain state. Because the strain rate here is significantly lower than in the offshore segment, this may eventually lead to different observed vertical motions on the coast.

5.1.2 Outlook

In this research, establishing the analog seismotectonic model enabled us to tackle a few seismotectonic problems of the shallow portion of the subduction zone at different time scales independently and jointly. For the short-term scale seismotectonic challenges (i.e., coseismic and postseismic intervals), the viscoelastic material could be involved in the system. This may help to enhance our understanding of how viscoelastic relaxation may slow down the elastic rebound of the upper plate and slab in the early stage of postseismic interval and stress transfer.

Currently, the analog velocity-weakening material in our laboratory can only mimic large and small fast earthquakes. Under the assumption that slow slip events are governed by rate-and-state-dependent friction, appropriate analog material could be tested and employed to mimic slow-slip events (SSEs). At the short-term scale, adding this material to the subduction megathrust interface may help us reveal the effect of the slow slip events on stress drop on the interface and, consequently, megathrust event triggering. At the long-term scale, the role of SSEs as a possible mechanism involved in the long-term uplift of the coastal region might be uncovered.

One of the key open questions in the earthquake geoscientists community is the interaction between upper plate faults and megathrust earthquakes as how one may trigger the other. As shown in this research, the discontinuities (i.e., upper plate faults) in the elastoplastic wedge can perturb the stress state in the upper plate. Hence, designing different configurations of analog seismotectonic experiments and monitoring the stress transfer via a high-resolution monitoring system may shed light on this interaction.

Although I have demonstrated how the strain pattern in the upper plate can be segmented in the trench-normal direction, trench-parallel strain pattern alteration is still under investigation. I am currently designing the trench-parallel heterogeneous interface configuration (velocity-weakening segment/creeping segment/velocity-weakening segment) in the HelTec analog laboratory at GFZ-Potsdam. The aim is to unwrap the

incremental and cumulative strain pattern over a single (coseismic and interseismic) and many seismic cycles. This may help geodesists and geologists to interpret the trench-parallel inconsistency and alteration in horizontal and vertical surface velocities and uplift patterns along the coastal region.

6 Curriculum Vitae

For reasons of data protection, the curriculum vitae is not published in the electronic version.